

# CLUSTER ALGEBRA AND COMPLEX VOLUME OF ONCE-PUNCTURED TORUS BUNDLES AND TWO-BRIDGE LINKS

KAZUHIRO HIKAMI AND REI INOUE

ABSTRACT. We propose a method to compute complex volume of 2-bridge link complements. Our construction sheds light on a relationship between cluster variables with coefficients and canonical decompositions of link complements.

## 1. Introduction

The cluster algebra was introduced by Fomin and Zelevinsky in [8], and it has been studied extensively since then. The characteristic operation in the cluster algebra called “mutation” is related to various notions, and there exist many applications of cluster algebra to the representation theory of Lie algebras and quantum groups, triangulated surface [6, 7], Teichmüller theory [5], integrable systems, and so on.

In geometry, the cluster algebraic techniques are used to understand hyperbolic structure of fibered bundles [15], where cluster  $y$ -variables are identified with moduli of ideal hyperbolic tetrahedra. Our purpose in this paper is to study complex volume of 2-bridge link complements  $M$  via cluster variables with coefficients. The complex volume is a complexification of hyperbolic volume,

$$\text{Vol}(M) + i \text{CS}(M),$$

where  $\text{Vol}(M)$  is the hyperbolic volume and  $\text{CS}(M)$  is the Chern–Simons invariant of  $M$ . Based on canonical decompositions of 2-bridge link complements in [19], we clarify a relationship between ideal tetrahedra and cluster mutations. Main observation is that the cluster variable with coefficients is closely related to Zickert’s formulation of complex volume [23], and that the complex volume is given from the cluster variable (Theorem 4.9, also Remark 4.10). We shall also give a formula of complex volume for once-punctured torus bundle over the circle (Theorem 3.9).

There may be natural extensions of our results. One of them is a quantization of the cluster algebra, which will be helpful in studies of Volume Conjecture [12, 13], a relationship between hyperbolic geometry and quantum invariants. Indeed in the case of once-punctured torus bundle, a classical limit of adjoint action of mutations and its relationship with [3, 11] are studied in [20]. Also a generalization to higher rank [5] remains for future works.

This paper is organized as follows. In Section 2, we briefly review the definition of the cluster algebra and the three-dimensional hyperbolic geometry, and explain their interrelationship by taking a simple example. Section 3 is devoted to the once-punctured

torus bundles over the circle. We formulate the hyperbolic volume via  $y$ -variables, and the complex volume via cluster variables. Section 4 is for 2-bridge links. First we review a canonical decomposition of the 2-bridge link complements, and we reformulate it in terms of the cluster algebra. The key is to introduce the cluster coefficient as an element of the tropical semifield. We give an explicit formula for the complex volume in terms of the cluster variables.

## 2. Cluster Algebra and 3-Dimensional Hyperbolic Geometry

### 2.1 Cluster Algebra

We briefly give a definition of the cluster algebras following [8, 9]. See these papers for details. We let  $(\mathbb{P}, \oplus, \cdot)$  be a semifield with a multiplication  $\cdot$  and an addition  $\oplus$ . This means that  $(\mathbb{P}, \cdot)$  is an abelian multiplicative group endowed with a binary operation  $\oplus$  which is commutative, associative, and distributive with respect to the group multiplication  $\cdot$ . Let  $\mathbb{QP}$  denote the quotient field of the group ring  $\mathbb{ZP}$  of  $(\mathbb{P}, \cdot)$ . (Note that  $\mathbb{ZP}$  is an integral domain [8].) Fix  $N \in \mathbb{Z}_{>0}$ . Let  $\mathbb{QP}(\mathbf{u})$  be the rational functional field of algebraically independent variables  $\{u_k\}_{k=1, \dots, N}$ .

**Definition 2.1.** A seed is a triple  $(\mathbf{x}, \boldsymbol{\varepsilon}, \mathbf{B})$ , where

- a cluster  $\mathbf{x} = (x_1, \dots, x_N)$  is an  $N$ -tuple of elements in  $\mathbb{QP}(\mathbf{u})$  such that  $\{x_k\}_{k=1, \dots, N}$  is a free generating set of  $\mathbb{QP}(\mathbf{u})$ ,
- a coefficient tuple  $\boldsymbol{\varepsilon} = (\varepsilon_1, \dots, \varepsilon_N)$  is an  $N$ -tuple of elements in  $\mathbb{P}$ ,
- an exchange matrix  $\mathbf{B} = (b_{ij})$  is an  $N \times N$  skew symmetric integer matrix.

We call  $x_i$  a cluster variable, and  $\varepsilon_i$  a coefficient.

An important tool in the cluster algebra is a mutation, which relates cluster seeds.

**Definition 2.2.** Let  $(\mathbf{x}, \boldsymbol{\varepsilon}, \mathbf{B})$  be a seed. For each  $k = 1, \dots, N$ , we define the mutation of  $(\mathbf{x}, \boldsymbol{\varepsilon}, \mathbf{B})$  by  $\mu_k$  as

$$\mu_k(\mathbf{x}, \boldsymbol{\varepsilon}, \mathbf{B}) = (\tilde{\mathbf{x}}, \tilde{\boldsymbol{\varepsilon}}, \tilde{\mathbf{B}}),$$

where

- an  $N$ -tuple  $\tilde{\mathbf{x}} = (\tilde{x}_1, \dots, \tilde{x}_N)$  of elements in  $\mathbb{QP}(\mathbf{u})$  is

$$\tilde{x}_i = \begin{cases} x_i, & \text{for } i \neq k, \\ \frac{\varepsilon_k}{1 \oplus \varepsilon_k} \cdot \frac{1}{x_k} \prod_{j: b_{jk} > 0} x_j^{b_{jk}} + \frac{1}{1 \oplus \varepsilon_k} \cdot \frac{1}{x_k} \prod_{j: b_{jk} < 0} x_j^{-b_{jk}}, & \text{for } i = k, \end{cases} \quad (2.1)$$

- a coefficient tuple  $\tilde{\boldsymbol{\varepsilon}} = (\tilde{\varepsilon}_1, \dots, \tilde{\varepsilon}_N)$  is

$$\tilde{\varepsilon}_i = \begin{cases} \varepsilon_k^{-1}, & \text{for } i = k, \\ \varepsilon_i \left( \frac{\varepsilon_k}{1 \oplus \varepsilon_k} \right)^{b_{ki}}, & \text{for } i \neq k, b_{ki} \geq 0, \\ \varepsilon_i (1 \oplus \varepsilon_k)^{-b_{ki}}, & \text{for } i \neq k, b_{ki} \leq 0, \end{cases} \quad (2.2)$$

- a skew symmetric integral matrix  $\tilde{\mathbf{B}} = (\tilde{b}_{ij})$  is

$$\tilde{b}_{ij} = \begin{cases} -b_{ij}, & \text{for } i = k \text{ or } j = k, \\ b_{ij} + \frac{1}{2} (|b_{ik}| b_{kj} + b_{ik} |b_{kj}|), & \text{otherwise.} \end{cases} \quad (2.3)$$

Note that the resulted triple  $(\tilde{\mathbf{x}}, \tilde{\boldsymbol{\varepsilon}}, \tilde{\mathbf{B}})$  is again a seed. We remark that  $\mu_k$  is involutive, and that  $\mu_j$  and  $\mu_k$  are commutative if and only if  $b_{jk} = b_{kj} = 0$ .

By starting from an initial seed  $(\mathbf{x}, \boldsymbol{\varepsilon}, \mathbf{B})$ , we iterate mutations and collect all obtained seeds. The cluster algebra  $\mathcal{A}(\mathbf{x}, \boldsymbol{\varepsilon}, \mathbf{B})$  is the  $\mathbb{Z}\mathbb{P}$ -subalgebra of the rational function field  $\mathbb{Q}\mathbb{P}(\mathbf{u})$  generated by all the cluster variables. In fact, in this paper we do not need the cluster algebra itself, but the seeds and the mutations. Further, we use the following:

**Proposition 2.3** ([9]). *For a seed  $(\mathbf{x}, \boldsymbol{\varepsilon}, \mathbf{B})$ , let  $\mathbf{y}$  be an  $N$ -tuple  $\mathbf{y} = (y_1, \dots, y_N)$  in  $\mathbb{Q}\mathbb{P}(\mathbf{u})$  defined as*

$$y_j = \varepsilon_j \prod_k x_k^{b_{kj}}. \quad (2.4)$$

Then the mutation of  $(\mathbf{x}, \boldsymbol{\varepsilon}, \mathbf{B})$  in Def. 2.2 induces a mutation of a pair  $(\mathbf{y}, \mathbf{B})$ ,

$$\mu_k(\mathbf{y}, \mathbf{B}) = (\tilde{\mathbf{y}}, \tilde{\mathbf{B}}), \quad (2.5)$$

where

- $\tilde{\mathbf{y}} = (\tilde{y}_1, \dots, \tilde{y}_N)$  is analogous to (2.2),

$$\tilde{y}_i = \begin{cases} y_k^{-1}, & \text{for } i = k, \\ y_i \left( \frac{y_k}{1 + y_k} \right)^{b_{ki}}, & \text{for } i \neq k, b_{ki} \geq 0, \\ y_i (1 + y_k)^{-b_{ki}}, & \text{for } i \neq k, b_{ki} \leq 0, \end{cases} \quad (2.6)$$

- $\tilde{\mathbf{B}} = (\tilde{b}_{ij})$  is (2.3).

This proposition holds for an arbitrary semifield  $(\mathbb{P}, \oplus, \cdot)$ . In this paper we call  $y_i$  a cluster  $y$ -variable, or a  $y$ -variable. Hereafter we use the following tropical semifield [9].

**Definition 2.4.** Set  $\mathbb{P} = \{\delta^k \mid k \in \mathbb{Z}\}$ . Let  $(\mathbb{P}, \oplus, \cdot)$  be a semifield generated by a variable  $\delta$  with a multiplication  $\cdot$  and an addition  $\oplus$ ,

$$\delta^{k_1} \oplus \delta^{k_2} = \delta^{\min(k_1, k_2)}. \quad (2.7)$$

**Definition 2.5.** We define a map  $\psi : \mathbb{P} \rightarrow \{-1, 1\}$ , given by substituting  $\delta = -1$  in elements of  $\mathbb{P}$ .

For the later use, we introduce the permutation acting on seeds.

**Definition 2.6.** For  $i, j \in \{1, \dots, N\}$  and  $i \neq j$ , let  $s_{i,j}$  be a permutation of subscripts  $i$  and  $j$  in seeds. For example a permuted cluster  $s_{i,j}(\mathbf{x})$  is defined by

$$s_{i,j}(\cdots, x_i, \cdots, x_j, \cdots) = (\cdots, x_j, \cdots, x_i, \cdots).$$

Actions on  $\boldsymbol{\varepsilon}$  and  $\mathbf{B}$  are defined in the same manner. They induce an action on  $\mathbf{y}$ , and  $s_{i,j}(\mathbf{y})$  has a same form.

## 2.2 Hyperbolic Geometry

A fundamental object in the three-dimensional hyperbolic geometry is an ideal hyperbolic tetrahedron  $\Delta$  in Fig. 1 [21]. The tetrahedron is parameterized by a modulus  $z \in \mathbb{C}$ , and each dihedral angle is given as in the figure. We mean  $z'$  and  $z''$  for given modulus  $z$  by

$$z' = 1 - \frac{1}{z}, \quad z'' = \frac{1}{1 - z}. \quad (2.8)$$

The cross section by the horosphere at each vertex is similar to the triangle in  $\mathbb{C}$  with vertices 0, 1, and  $z$  as in Fig. 2. In Fig. 1, we give an orientation to tetrahedron by assigning a vertex ordering [23], which is crucial in computing the complex volume of tetrahedra modulo  $\pi^2$ .

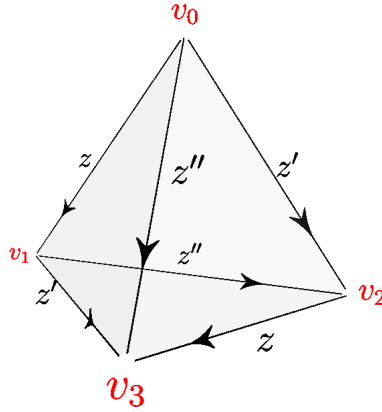


FIGURE 1. An ideal hyperbolic tetrahedron  $\Delta$  with modulus  $z$ . All 4 vertices are on  $\partial\mathbb{H}^3$ , and edges are geodesics in  $\mathbb{H}^3$ . Dihedral angles between pairs of faces are parametrized by  $z$ ,  $z' = 1 - 1/z$ , and  $z'' = 1/(1 - z)$ . To each vertex, we give a vertex ordering  $v_0, v_1, v_2$ , and  $v_3$ . Then an orientation of  $\Delta$  is induced when we give an orientation to an edge from  $v_a$  to  $v_b$  ( $a < b$ ).

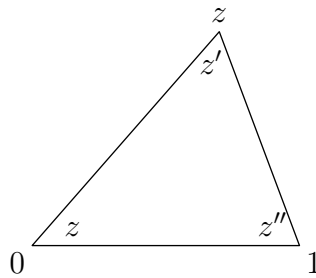


FIGURE 2. A triangle in  $\mathbb{C}$  with vertices 0, 1, and  $z$ .

The hyperbolic volume of an ideal tetrahedron  $\Delta$  with modulus  $z$  is given by the Bloch–Wigner function

$$D(z) = \operatorname{Im} \operatorname{Li}_2(z) + \arg(1 - z) \log |z|. \quad (2.9)$$

Here  $\operatorname{Li}_2(z)$  is the dilogarithm function,

$$\operatorname{Li}_2(z) = \sum_{n=1}^{\infty} \frac{z^n}{n^2},$$

for  $|z| < 1$ , and the analytic continuation for  $z \in \mathbb{C} \setminus [1, \infty)$  is given by

$$\operatorname{Li}_2(z) = - \int_0^z \log(1-s) \frac{ds}{s}.$$

Note that

$$\begin{aligned} D(z) &= D(z') = D(z'') \\ &= -D(1/z) = -D(1/z') = -D(1/z''). \end{aligned} \quad (2.10)$$

See, *e.g.*, [22] for details of the dilogarithm function.

We study the case that a cusped hyperbolic 3-manifold  $M$  is triangulated into a set of ideal tetrahedra  $\{\Delta_\nu\}$ . It is known that the modulus  $z_\nu$  of each ideal tetrahedron  $\Delta_\nu$  is determined from two conditions. One is a set of gluing equations, which means that dihedral angles around each edge sum up to  $2\pi$ . Another is a cusp condition so that  $M$  has a complete hyperbolic structure. Then the hyperbolic volume of  $M$  is given by

$$\operatorname{Vol}(M) = \sum_{\nu} D(z_\nu). \quad (2.11)$$

See [16, 18, 21] for details.

The complex volume,  $\operatorname{Vol}(M) + i \operatorname{CS}(M)$ , of  $M$  is a complexification of (2.11), and in view of the Bloch–Wigner function  $D(z)$  (2.9), it is natural to study the dilogarithm function  $\operatorname{Li}_2(z)$ . Although, in contrast to  $D(z)$ , the dilogarithm function  $\operatorname{Li}_2(z)$  is a multi-valued function, and we need a “flattening”, *i.e.*, the moduli of ideal tetrahedra with additional parameters  $p$  and  $q$ .

**Definition 2.7** ([17]). A flattening of an ideal tetrahedron  $\Delta$  is

$$(w_0, w_1, w_2) = (\log z + p\pi i, -\log(1-z) + q\pi i, \log(1-z) - \log z - (p+q)\pi i), \quad (2.12)$$

where  $z$  is the modulus of  $\Delta$  and  $p, q \in \mathbb{Z}$ . We use  $(z; p, q)$  to denote the flattening of  $\Delta$ .

By use of the flattening  $(z; p, q)$ , we introduce [16] an extended Rogers dilogarithm function by

$$\widehat{L}(z; p, q) = \operatorname{Li}_2(z) + \frac{1}{2} \log z \log(1-z) + \frac{\pi i}{2} (q \log z + p \log(1-z)) - \frac{\pi^2}{6}, \quad (2.13)$$

where  $p, q \in \mathbb{Z}$ . Here and hereafter, we mean the principal branch in the logarithm. In [17], the extended pre-Bloch group is defined as the free abelian group on the flattenings subject to a lifted five-term relation, and it is shown that the complex volume can be given as follows.

**Proposition 2.8** ([17]). *The complex volume of  $M$  is*

$$i (\operatorname{Vol}(M) + i \operatorname{CS}(M)) = \sum_{\nu} \operatorname{sgn}(\nu) \widehat{L}(z_\nu; p_\nu, q_\nu) \pmod{\pi^2}, \quad (2.14)$$

where  $(z_\nu; p_\nu, q_\nu)$  is a flattening of  $\Delta_\nu$ , and  $\operatorname{sgn}(\nu)$  is 1 (*resp.*  $-1$ ) when the orientation of  $\Delta_\nu$  is same with (*resp.* opposite to) that of  $\Delta$  in Fig. 1.

Zickert clarified that the flattening  $(z; p, q)$  can be given by complex parameters assigned to the edges of an ideal tetrahedron in the following way.

**Proposition 2.9** ([23]). *For the ideal tetrahedron  $\Delta$  in Fig. 1, let  $c_{ab}$  be a complex parameter on the edge connecting vertices  $v_a$  and  $v_b$  for  $0 \leq a < b \leq 3$ . When these complex parameters satisfy*

$$\frac{c_{03} c_{12}}{c_{02} c_{13}} = \pm z, \quad \frac{c_{01} c_{23}}{c_{03} c_{12}} = \pm \left(1 - \frac{1}{z}\right), \quad \frac{c_{02} c_{13}}{c_{01} c_{23}} = \pm \frac{1}{1-z}, \quad (2.15)$$

the flattening  $(z; p, q)$  is given by

$$\begin{aligned} \log z + p \pi i &= \log c_{03} + \log c_{12} - \log c_{02} - \log c_{13}, \\ -\log(1-z) + q \pi i &= \log c_{02} + \log c_{13} - \log c_{01} - \log c_{23}. \end{aligned} \quad (2.16)$$

In gluing tetrahedra to construct a three-manifold  $M$ , edges identified in  $M$  are required to have the same complex numbers.

*Remark 2.10.* It was demonstrated in [23] that these complex parameters  $c_{ab}$  can be read from a developing map such as Figs. 8 and 13. To summarize, when we have a triangulation  $\{\Delta_\nu\}$  with modulus  $z_\nu$  of a hyperbolic 3-manifold  $M$ , the flattening  $(z_\nu; p_\nu, q_\nu)$  can be given from the above with edge parameters  $c_{ab}$ , and we get the complex volume of  $M$  from (2.14).

### 2.3 Interrelationship

Correspondence between the cluster algebra and the hyperbolic geometry can be seen in a simple example.<sup>1</sup> We study a triangulated surface and its flip as in Fig. 3. A triangulation is related to a quiver, *i.e.*, a directed graph, where the number of edges in the triangulation is equal to the fixed number  $N$  in the cluster algebra [6]. A flip can be regarded as a cluster mutation, as depicted in the figure. Note that the exchange matrix  $\mathbf{B} = (b_{ij})$  can be read from the quiver by

$$b_{ij} = \#\{\text{arrows from } i \text{ to } j\} - \#\{\text{arrows from } j \text{ to } i\}.$$

By definition (2.4), the mutation  $\mu_3(\mathbf{y}, \mathbf{B}) = (\tilde{\mathbf{y}}, \tilde{\mathbf{B}})$ , is explicitly written as

$$\begin{aligned} \tilde{y}_1 &= y_1 (1 + y_3), \\ \tilde{y}_2 &= y_2 (1 + y_3^{-1})^{-1}, \\ \tilde{y}_3 &= y_3^{-1}, \\ \tilde{y}_4 &= y_4 (1 + y_3^{-1})^{-1}, \\ \tilde{y}_5 &= y_5 (1 + y_3). \end{aligned} \quad (2.17)$$

On the other hand, we may regard the flip in Fig. 3 as an attachment of an ideal tetrahedron  $\Delta$  with modulus  $z$  whose faces are pleated. See Fig. 4. When we denote by  $z_k$  the dihedral angle on edge  $k$  labeled as in Fig. 3, a dihedral angle  $\tilde{z}_k$  after attaching

---

<sup>1</sup>We thank T. Dimofte.

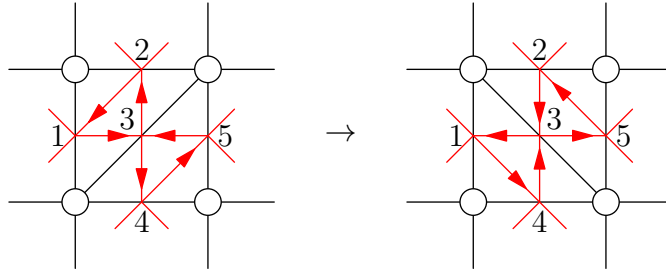


FIGURE 3. A flip of a triangulated punctured surface. Also depicted are the quivers associated to the triangulated surfaces.

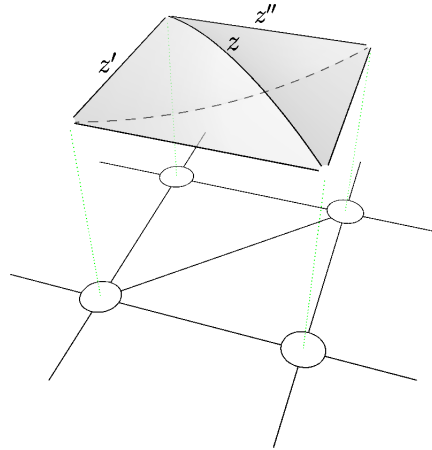


FIGURE 4. A flip and an attachment of pleated ideal tetrahedron.

$\Delta$  is given by

$$\begin{aligned}
 \tilde{z}_1 &= z_1 z', \\
 \tilde{z}_2 &= z_2 z'', \\
 \tilde{z}_3 &= z, \\
 \tilde{z}_4 &= z_4 z'', \\
 \tilde{z}_5 &= z_5 z',
 \end{aligned}
 \tag{2.18}$$

with a hyperbolic gluing condition

$$z_3 z = 1.$$

Comparing (2.17) with (2.18), we observe that the cluster  $y$ -variable is related to the dihedral angle by

$$y_k = -z_k,$$

and especially a modulus of the ideal tetrahedron  $\Delta$  is given by

$$z = -\frac{1}{y_3}.$$
(2.19)

See that a subscript “3” denotes a label of vertex in the quiver where the mutation ( $\mu_3$ ) was applied.

Our idea on a geometrical role of the cluster variable  $x_k$  is as follows. We know from (2.4) that the  $y$ -variable is written as

$$y_3 = \varepsilon_3 \frac{x_1 x_5}{x_2 x_4}.$$

We also see from (2.1) that the mutation  $\mu_3$  sends a cluster variable  $x_3$  to

$$\tilde{x}_3 = \frac{\varepsilon_3}{1 \oplus \varepsilon_3} \cdot \frac{x_1 x_5}{x_3} + \frac{1}{1 \oplus \varepsilon_3} \cdot \frac{x_2 x_4}{x_3},$$

where we take the tropical semifield of Def. 2.4. Thus, using (2.19) we get

$$z = -\frac{1}{\varepsilon_3} \cdot \frac{x_2 x_4}{x_1 x_5}, \quad \frac{1}{1-z} = \frac{\varepsilon_3}{1 \oplus \varepsilon_3} \cdot \frac{x_1 x_5}{\tilde{x}_3 x_3}.$$

When we apply the map  $\psi$  in Def. 2.5 to the above, the coefficient parts including  $\varepsilon_3$  are  $\pm 1$ . By comparing these formulae with (2.15), we notice that the cluster variables  $x_i$  play a role of Zickert's parameters  $c_{ab}$ .

### 3. Once-Punctured Torus Bundle over $S^1$

#### 3.1 $y$ -pattern and Hyperbolic Volume

Let  $\Sigma_{1,1}$  be a once-punctured torus,  $(\mathbb{R}^2 \setminus \mathbb{Z}^2)/\mathbb{Z}^2$ . We set  $M_\varphi$  to be the once-punctured torus bundle over the circle, whose monodromy is determined by a mapping class  $\varphi \in SL(2; \mathbb{Z})$ . More precisely, via  $\varphi : \Sigma_{1,1} \rightarrow \Sigma_{1,1}$  we define an identification  $(x, 0) \sim (\varphi(x), 1)$  for  $\forall x \in \Sigma_{1,1}$ , and set  $M_\varphi = \Sigma_{1,1} \times [0, 1]/\sim$ . It is known that  $M_\varphi$  is hyperbolic when  $\varphi$  has distinct real eigenvalues. Up to conjugation we have

$$\varphi = R^{s_1} L^{t_1} \cdots R^{s_n} L^{t_n}, \quad (3.1)$$

where

$$R = \begin{pmatrix} 1 & 1 \\ 0 & 1 \end{pmatrix}, \quad L = \begin{pmatrix} 1 & 0 \\ 1 & 1 \end{pmatrix}.$$

To denote a mapping class (3.1) we use a sequence of symbols  $F_1 F_2 \cdots F_c = \underbrace{R \cdots R}_{s_1} \underbrace{L \cdots L}_{t_1} \cdots \underbrace{R \cdots R}_{s_n} \underbrace{L \cdots L}_{t_n}$  where  $F_k = R$  or  $L$ , and

$$c = \sum_{j=1}^n (s_j + t_j). \quad (3.2)$$

We use a triangulation of  $\Sigma_{1,1}$  as depicted in Fig. 5. It is related to the Farey triangles [4], which we will explain in Section 4.1. The actions of  $R$  and  $L$  are interpreted as ‘‘flips’’ of triangulation as shown in the figure. The triangulation is translated into the cluster algebra of  $N = 3$  with the exchange matrix as

$$\mathbf{B} = \begin{pmatrix} 0 & -2 & 2 \\ 2 & 0 & -2 \\ -2 & 2 & 0 \end{pmatrix}. \quad (3.3)$$



This denotes the quiver in Fig. 6, where each vertex has a labeling corresponding to that of an edge in the triangulation. Then the flips  $R$  and  $L$  can be identified with the mutations in the cluster algebra (cf. [20]), and we have

$$R = s_{1,3} \mu_1, \quad L = s_{2,3} \mu_2, \quad (3.4)$$

where  $s_{i,j}$  is the permutation defined in Def. 2.6. See Fig. 5. We have used the permutations so that the exchange matrix (3.3) is invariant under these actions. In this way the flips  $R$  and  $L$  act on the  $y$ -variable respectively as

$$(\mathbf{y}, \mathbf{B}) \xrightarrow{R} (R(\mathbf{y}), \mathbf{B}), \quad (\mathbf{y}, \mathbf{B}) \xrightarrow{L} (L(\mathbf{y}), \mathbf{B}), \quad (3.5)$$

where

$$R(\mathbf{y}) = \begin{pmatrix} y_3(1+y_1^{-1})^{-2} \\ y_2(1+y_1)^2 \\ y_1^{-1} \end{pmatrix}^\top, \quad L(\mathbf{y}) = \begin{pmatrix} y_1(1+y_2^{-1})^{-2} \\ y_3(1+y_2)^2 \\ y_2^{-1} \end{pmatrix}^\top. \quad (3.6)$$

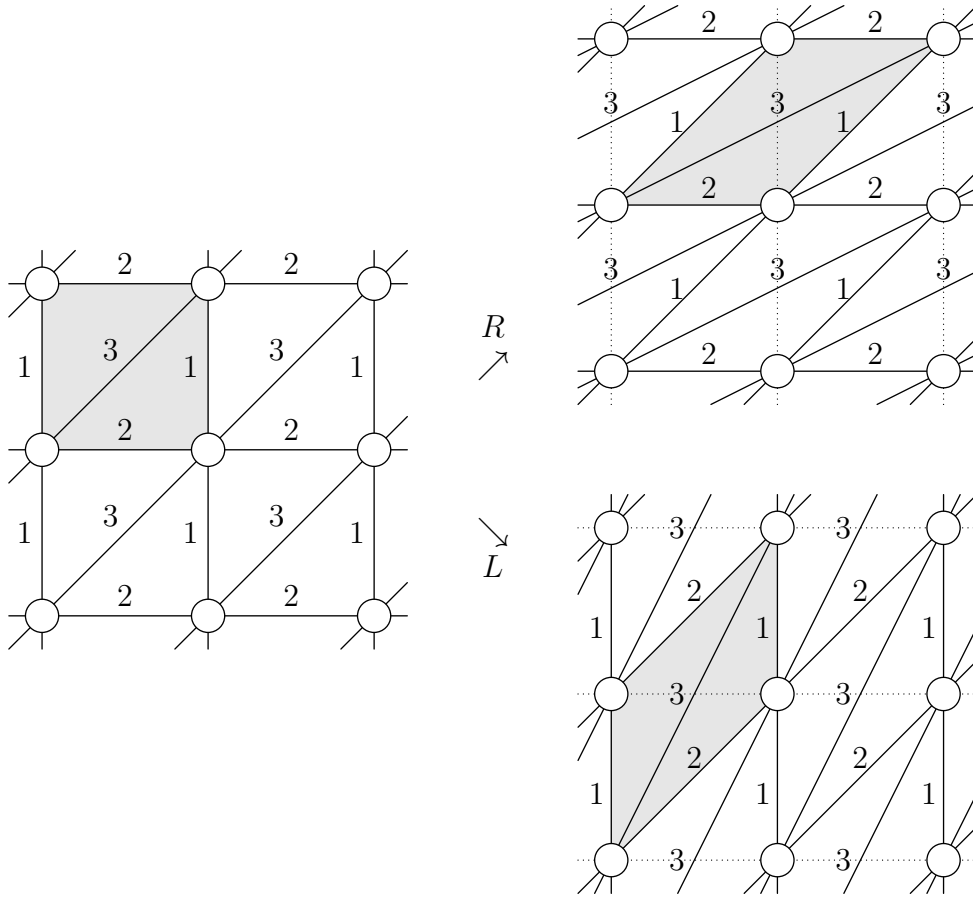


FIGURE 5. A triangulation of the once-punctured torus  $\Sigma_{1,1}$  (left). The vertex denotes a puncture. A fundamental region is colored gray. A labeling of each edge corresponds to that of each vertex in the quiver in Fig. 6. The actions of flips,  $R$  and  $L$ , are given in the right hand side.

**Definition 3.1.** A  $y$ -pattern of a mapping class  $\varphi = F_1 \cdots F_c$  (3.1) is  $\mathbf{y}[k]$  for  $k = 1, 2, \dots, c + 1$  defined recursively by

$$\mathbf{y}[k + 1] = F_k(\mathbf{y}[k]). \quad (3.7)$$

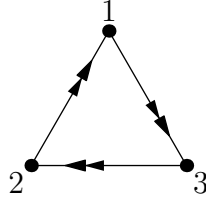


FIGURE 6. A quiver associated to a triangulation of the once-punctured torus  $\Sigma_{1,1}$  in the left figure in Fig. 5.

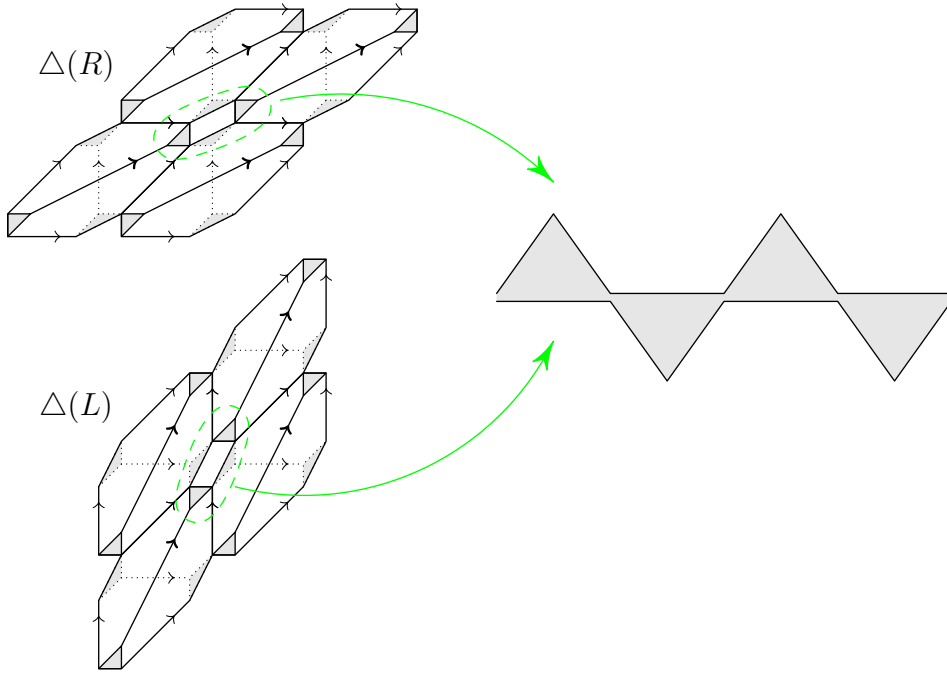


FIGURE 7. Left: The tetrahedra  $\Delta(R)$  and  $\Delta(L)$  assigned to the flips  $R$  and  $L$  on the once-punctured torus  $\Sigma_{1,1}$ . Once we fix an orientation of triangulation of  $\Sigma_{1,1}$ , an orientation of tetrahedra is induced as illustrated in the figure. Right: Drawn is a part of Euclidean triangulations of the cusp.

We have seen in Section 2.3 that the cluster mutation is interpreted as an attachment of an ideal tetrahedron. Thus to each flip  $F_k$ ,  $R$  or  $L$  defined in (3.4), we can assign a single ideal hyperbolic tetrahedron  $\Delta(F_k)$  as illustrated in Fig. 7. The triangulations of  $\Sigma_{1,1}$  in Fig. 5 can be regarded as the top and bottom pleated faces of ideal tetrahedron in Fig. 7 [4]. In a cross section by horosphere at a vertex we have four triangles, and each of them has one vertex not shared with any of the other three as in Fig. 7.

Our first claim is that the modulus of each ideal tetrahedron is given from a  $y$ -pattern. See also [15].

**Proposition 3.2.** *Let  $\mathbf{y}[k]$  be a  $y$ -pattern of  $\varphi$  with an initial condition,*

$$\mathbf{y}[1] = \left( y_1, y_2, \frac{1}{y_1 y_2} \right). \quad (3.8)$$

Here  $y_1$  and  $y_2$  are solutions of

$$\mathbf{y}[1] = \mathbf{y}[c + 1], \quad (3.9)$$

such that each modulus  $z[k]$  defined by

$$z[k] = \begin{cases} -\frac{1}{y[k]_1}, & \text{when } F_k = R, \\ -\frac{1}{y[k]_2}, & \text{when } F_k = L, \end{cases} \quad (3.10)$$

is in the upper half plane  $\mathbb{H}$  for  $k = 1, \dots, c$ . Then  $z[k]$  is the modulus of the tetrahedron  $\Delta(F_k)$ .

*Remark 3.3.* It is known [10] that there exists a geometric solution of (3.9), such that the imaginary part of  $z[k]$  is positive for all  $k$ .

**Corollary 3.4.** *The hyperbolic volume of  $M_\varphi$  is given by*

$$\text{Vol}(M_\varphi) = \sum_{k=1}^c D(z[k]), \quad (3.11)$$

where  $z[k]$  is the modulus of  $\Delta(F_k)$  given in (3.10).

### 3.2 Proof of Proposition 3.2

We have discussed in Section 2 that the cluster  $y$ -variable is related to the modulus of ideal tetrahedron. To prove that the  $y$ -pattern  $\mathbf{y}[k]$  given by (3.7) describes a complete hyperbolic structure of  $M_\varphi$ , we need to check [18, 21] that both gluing conditions and a completeness condition are fulfilled. The gluing conditions may be trivial once we know the fact in Section 2.3. Though, we need to check the gluing conditions at edges on top/bottom triangulated surfaces, and the completeness condition is far from trivial. In the following, we shall check all of them by use of a developing map of torus at infinity of  $M_\varphi$  (3.1), which is depicted in Fig. 8 (see, *e.g.*, [10]).

First of all, when  $s_1 \geq 2$ , we have

$$\begin{aligned} z[3] (z''[2])^2 z[1] &= \frac{-1}{y[3]_1} \left( \frac{1}{1 + y[2]_1^{-1}} \right)^2 \frac{-1}{y[1]_1} \\ &= \frac{-1}{y[2]_3} \frac{-1}{y[1]_1} = 1. \end{aligned}$$

Here we have used  $\mathbf{y}[3] = R(\mathbf{y}[2])$  in the second equality, and the last equality follows from  $\mathbf{y}[2] = R(\mathbf{y}[1])$ . See (3.6) for the action of flip  $R$ . We see that this equality is nothing but a gluing condition for the second circle from the bottom in Fig. 8. A case of  $s_1 = 1$  can be checked in the similar manner.

In the same manner, we can check

$$z[k+1] (z''[k])^2 z[k-1] = 1,$$

for  $2 \leq k \leq c-1$ , which also corresponds to a gluing condition in the figure. Using the periodic condition (3.9), we have

$$\begin{aligned} z[2] (z''[1])^2 z[c] &= \frac{-1}{y[2]_1} \left( \frac{1}{1 + y[1]_1^{-1}} \right)^2 \frac{-1}{y[c]_2} \\ &= 1, \end{aligned}$$

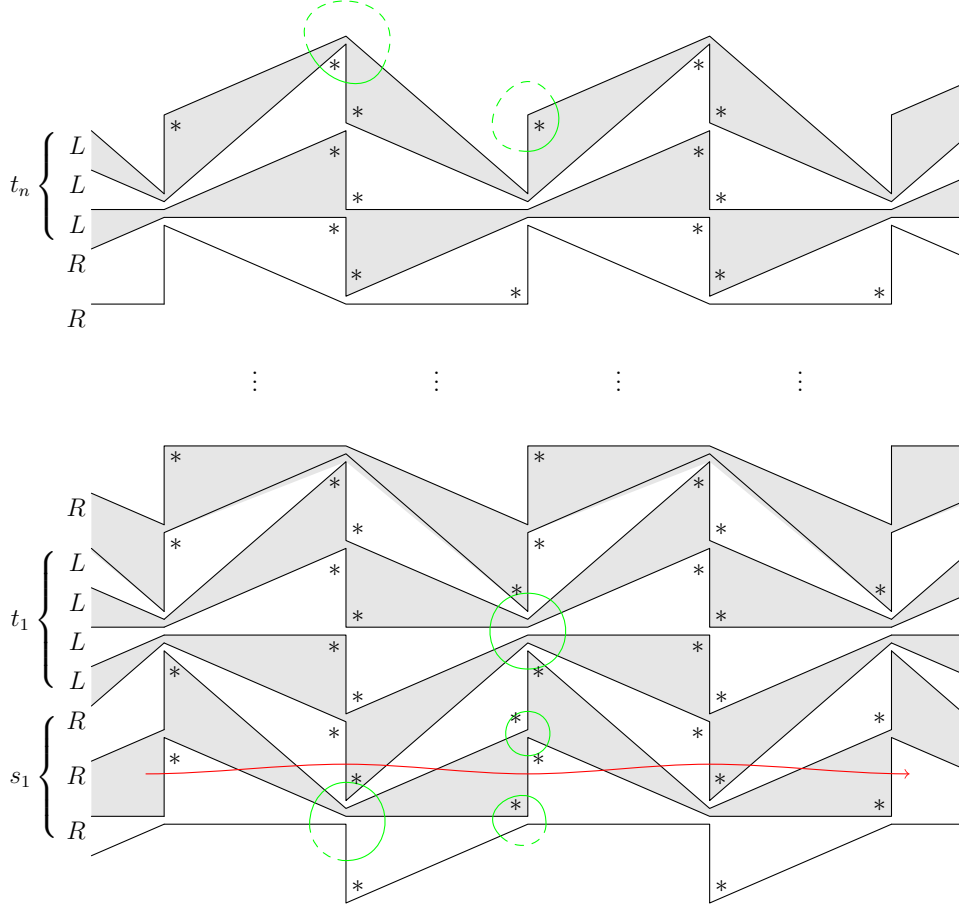


FIGURE 8. The developing map of the once-punctured torus bundle over the circle  $M_\varphi$ . Here  $R$  and  $L$  respectively denote the ideal tetrahedron  $\triangle(R)$  and  $\triangle(L)$  in Fig. 7. To emphasize the layered structure, every vertex is opened up and each layer is colored alternately. See Fig. 7. We denote dihedral angles  $z[k]$  by  $*$ .

where we have used  $y[1]_3 = y[c+1]_3 = y[c]_2^{-1}$ . This coincides with a consistency condition for the right semi-circle (top and bottom) in the figure.

We can further check that

$$\begin{aligned} z[s_1+1] \cdot \prod_{k=1}^{s_1} (z'[k])^2 \cdot (z'[c])^2 z[c-1] &= \frac{-1}{y[s_1+1]_2} \cdot \prod_{k=1}^{s_1} (1+y[k]_1)^2 \cdot (1+y[c]_2)^2 \frac{-1}{y[c-1]_2} \\ &= \frac{1}{y[1]_2} y[c+1]_2 = 1, \end{aligned}$$

due to (3.9). This identity corresponds to a gluing condition for the left semi-circle (top and bottom) in the figure. As another example of this type of equality, we have

$$z[s_1+t_1+1] \cdot \prod_{k=s_1}^{s_1+t_1} (z''[k])^2 \cdot z[s_1-1] = 1,$$

which denotes a gluing condition for the right middle large circle. In this way, it is straightforward to check consistency conditions in the figure.

A completeness condition can be checked similarly. We have

$$\begin{aligned} \left( \frac{1}{z[1]} \frac{z'[2]}{z''[2]} \cdot \prod_{k=3}^{s_1} (z'[k])^2 \cdot z[s_1 + 1] \right)^2 &= \left( \frac{y[1]_1}{y[2]_1} \cdot \prod_{k=2}^{s_1} (1 + y[k]_1)^2 \cdot \frac{1}{y[s_1 + 1]_2} \right)^2 \\ &= \left( \frac{1}{y[1]_1 y[1]_2 y[1]_3} \right)^2 = 1, \end{aligned}$$

where the last equality follows from the initial condition (3.8). We can see that this equality denotes a completeness condition from the curve in the figure.

This completes the proof.

### 3.3 Cluster Pattern and Complex Volume

In the previous Section 3.2, we have proved that the  $y$ -variables give the hyperbolic volume of the manifold  $M_\varphi$ . We shall discuss that the cluster variables give the *complex volume* of  $M_\varphi$ .

We reformulate the preceding result in Section 3.2 by use of cluster variables with coefficients. By definition, the permuted mutations  $R$  and  $L$  (3.4) act on a seed respectively as

$$(\mathbf{x}, \boldsymbol{\varepsilon}, \mathbf{B}) \xrightarrow{R} (R(\mathbf{x}, \boldsymbol{\varepsilon}), \mathbf{B}), \quad (\mathbf{x}, \boldsymbol{\varepsilon}, \mathbf{B}) \xrightarrow{L} (L(\mathbf{x}, \boldsymbol{\varepsilon}), \mathbf{B}). \quad (3.12)$$

where

$$\begin{aligned} R(\mathbf{x}, \boldsymbol{\varepsilon}) &= \left( \left( \begin{array}{ccc} x_3 & & \\ & x_2 & \\ \frac{\varepsilon_1}{1 \oplus \varepsilon_1} \frac{x_2^2}{x_1} + \frac{1}{1 \oplus \varepsilon_1} \frac{x_3^2}{x_1} & & \end{array} \right)^\top, \left( \begin{array}{c} \varepsilon_3 \left( \frac{\varepsilon_1}{1 \oplus \varepsilon_1} \right)^2 \\ \varepsilon_2 (1 \oplus \varepsilon_1)^2 \\ \varepsilon_1^{-1} \end{array} \right)^\top \right), \\ L(\mathbf{x}, \boldsymbol{\varepsilon}) &= \left( \left( \begin{array}{ccc} x_1 & & \\ & x_3 & \\ \frac{1}{1 \oplus \varepsilon_2} \frac{x_1^2}{x_2} + \frac{\varepsilon_2}{1 \oplus \varepsilon_2} \frac{x_3^2}{x_2} & & \end{array} \right)^\top, \left( \begin{array}{c} \varepsilon_1 \left( \frac{\varepsilon_2}{1 \oplus \varepsilon_2} \right)^2 \\ \varepsilon_3 (1 \oplus \varepsilon_2)^2 \\ \varepsilon_2^{-1} \end{array} \right)^\top \right). \end{aligned} \quad (3.13)$$

**Definition 3.5.** A cluster pattern of  $\varphi = F_1 \cdots F_c$  (3.1) is  $(\mathbf{x}[k], \boldsymbol{\varepsilon}[k])$  for  $k = 1, 2, \dots, c+1$  defined recursively by

$$(\mathbf{x}[k+1], \boldsymbol{\varepsilon}[k+1]) = F_k(\mathbf{x}[k], \boldsymbol{\varepsilon}[k]). \quad (3.14)$$

We set an initial seed  $(\mathbf{x}, \boldsymbol{\varepsilon}, \mathbf{B})$  by

$$\mathbf{x}[1] = (x_1, x_2, x_3), \quad \boldsymbol{\varepsilon}[1] = (1, 1, 1), \quad (3.15)$$

and (3.3). Note that for all  $k$  we have

$$\boldsymbol{\varepsilon}[k] = (1, 1, 1). \quad (3.16)$$

When we set a periodic condition

$$\mathbf{x}[c+1] = \mathbf{x}[1], \quad (3.17)$$

all cluster variables  $x[k]_j$  are determined up to constant. Thanks to Prop. 2.3 with (3.3), the  $y$ -pattern in Prop. 3.2 can be identified with

$$\mathbf{y}[k] = \left( \left( \frac{x[k]_2}{x[k]_3} \right)^2, \left( \frac{x[k]_3}{x[k]_1} \right)^2, \left( \frac{x[k]_1}{x[k]_2} \right)^2 \right), \quad (3.18)$$

and (3.17) supports the periodicity of  $y$ -variable,  $\mathbf{y}[1] = \mathbf{y}[c+1]$ . We choose  $\mathbf{x}[k]$  such that the  $y$ -variable (3.18) is a geometric solution of (3.9). As was shown in Section 2.3, the cluster variable  $\mathbf{x}[k]$  can be regarded as Zickert's edge parameters  $c_{ab}$  of  $\Delta(F_k)$ . See Remark 2.10.

To get the complex volume modulo  $\pi^2$ , we need to take into account of the orientation of  $\Delta(F_k)$ . When we assign an orientation to the triangulations of  $\Sigma_{1,1}$ , it induces an orientations of  $\Delta(F_k)$  as illustrated in Fig. 7 [17]. The tetrahedron  $\Delta(R)$  has the same orientation with  $\Delta$  in Fig. 1, while the tetrahedron  $\Delta(L)$  has the opposite orientation. Using a relationship between the vertex ordering and dihedral angles in Fig. 1, we obtain the following.

**Lemma 3.6.** *Let  $\mathbf{x}[k]$  be a cluster pattern satisfying the condition (3.17). Then the modulus  $z[k]$  of  $\Delta(F_k)$  is given by*

$$z[k] = \begin{cases} \frac{x[k]_1 x[k+1]_3}{(x[k]_3)^2}, & \text{for } F_k = R, \\ \frac{x[k]_2 x[k+1]_3}{(x[k]_3)^2}, & \text{for } F_k = L, \end{cases} \quad (3.19)$$

for  $k = 1, \dots, c$ .

*Proof.* When  $F_k = R$ , we see from the vertex ordering of  $\Delta(R)$  in Fig. 7 and  $\Delta$  in Fig. 1 that  $-1/y[k]_1$  is identified with  $z''[k]$ . By using (3.13) and (3.18), we obtain

$$z[k] = 1 + y[k]_1 = \frac{(x[k]_2)^2 + (x[k]_3)^2}{(x[k]_3)^2} = \frac{x[k]_1 x[k+1]_3}{(x[k]_3)^2}.$$

When  $F_k = L$ , we find that  $\Delta(L)$  in Fig. 7 has an opposite vertex ordering to  $\Delta$  in Fig. 1. Thus  $(-1/y[k]_2)^{-1}$  corresponds to  $z''[k]$ , and we get

$$z[k] = 1 + \frac{1}{y[k]_2} = \frac{(x[k]_1)^2 + (x[k]_3)^2}{(x[k]_3)^2} = \frac{x[k]_2 x[k+1]_3}{(x[k]_3)^2}.$$

□

*Remark 3.7.* Due to orientation of the tetrahedron, a solution is geometric if and only if  $\text{Im } z[k] > 0$  (resp.  $\text{Im } z[k] < 0$ ) for  $F_k = R$  (resp.  $F_k = L$ ).

We obtain the flattening of  $\Delta(F_k)$  as follows.

**Lemma 3.8.** *We follow the setting at Lemma 3.6. The flattening  $(z[k]; p[k], q[k])$  for the tetrahedron  $\Delta(F_k)$  is given by*

$$\begin{aligned} \log z[k] + p[k] \pi i &= \begin{cases} \log x[k]_1 + \log x[k+1]_3 - 2 \log x[k]_3, & \text{for } F_k = R, \\ \log x[k]_2 + \log x[k+1]_3 - 2 \log x[k]_3, & \text{for } F_k = L, \end{cases} \\ -\log(1 - z[k]) + q[k] \pi i &= \begin{cases} 2 \log x[k]_3 - 2 \log x[k]_2, & \text{for } F_k = R, \\ 2 \log x[k]_3 - 2 \log x[k]_1, & \text{for } F_k = L, \end{cases} \end{aligned} \quad (3.20)$$

for  $k = 1, \dots, c$ .

*Proof.* We recall that the moduli is given in (3.19), and that the flips have the actions in (3.13). Then we obtain

$$\frac{1}{1 - z[k]} = \begin{cases} -\left(\frac{x[k]_3}{x[k]_2}\right)^2, & \text{for } F_k = R, \\ -\left(\frac{x[k]_3}{x[k]_1}\right)^2, & \text{for } F_k = L. \end{cases} \quad (3.21)$$

From (3.19), (3.21), and Zickert's identity (2.15), the claim follows.  $\square$

As a consequence of Lemma 3.6 and Lemma 3.8, it is straightforward to obtain the following theorem, which is the main result in this section.

**Theorem 3.9.** *The complex volume of  $M_\varphi$  is*

$$i (\text{Vol}(M_\varphi) + i \text{CS}(M_\varphi)) = \sum_{k=1}^c \text{sgn}(F_k) \widehat{L}(z[k]; p[k], q[k]) \pmod{\pi^2}, \quad (3.22)$$

where  $\text{sgn}(R) = 1$  and  $\text{sgn}(L) = -1$ , and the flattening  $(z[k]; p[k], q[k])$  is given in (3.19) and (3.20).

*Remark 3.10.* When we discard the vertex ordering of the ideal hyperbolic tetrahedra  $\Delta(F_k)$ , the resulting complex volume is defined modulo  $\frac{\pi^2}{6}$  [17]. Ignoring orientations of  $\Delta(F_k)$ , we may simply set the moduli of tetrahedra from (3.10) and (3.18) as

$$z[k] = \begin{cases} -\left(\frac{x[k]_3}{x[k]_2}\right)^2, & \text{for } F_k = R, \\ -\left(\frac{x[k]_1}{x[k]_3}\right)^2, & \text{for } F_k = L, \end{cases}$$

for  $k = 1, \dots, c$ . Then we obtain the flattening  $(z[k]; p[k], q[k])$  of  $\Delta(F_k)$  from

$$\begin{aligned} \log z[k] + p[k] \pi i &= \begin{cases} 2 \log x[k]_3 - 2 \log x[k]_2, & \text{for } F_k = R, \\ 2 \log x[k]_1 - 2 \log x[k]_3, & \text{for } F_k = L, \end{cases} \\ -\log(1 - z[k]) + q[k] \pi i &= \begin{cases} 2 \log x[k]_2 - \log x[k]_1 - \log x[k+1]_3, & \text{for } F_k = R, \\ 2 \log x[k]_3 - \log x[k]_2 - \log x[k+1]_3, & \text{for } F_k = L. \end{cases} \end{aligned}$$

With these flattening, we have the complex volume modulo  $\frac{\pi^2}{6}$  [17] by

$$i (\text{Vol}(M_\varphi) + i \text{CS}(M_\varphi)) = \sum_{k=1}^c \widehat{L}(z[k]; p[k], q[k]) \pmod{\frac{\pi^2}{6}}.$$

### 3.4 Example: $RL^2$

We take an example  $\varphi = RL^2$ . A cluster pattern is

$$\mathbf{x}[1] \xrightarrow{R} \mathbf{x}[2] \xrightarrow{L} \mathbf{x}[3] \xrightarrow{L} \mathbf{x}[4].$$

An initial cluster variable  $\mathbf{x}[1] = (x_1, x_2, x_3)$  is solved up to constant from the periodic condition (3.17),  $\mathbf{x}[1] = \mathbf{x}[4]$ :

$$x_1 = x_3, \quad \left(\frac{x_2}{x_3}\right)^4 + \left(\frac{x_2}{x_3}\right)^2 + 2 = 0.$$

By setting  $x_1 = x_3 = 1$ , geometric solutions are  $x_2 = \pm(0.6760 \cdots + i \cdot 0.9783 \cdots)$ . From (3.20) the solution with plus sign gives the flattening parameters  $(p[k], q[k])$  for  $k = 1, 2, 3$  as  $(0, -1)$ ,  $(0, 1)$ ,  $(0, 1)$ , while the minus sign solution gives  $(0, 1)$ ,  $(-2, 1)$ ,  $(2, -1)$ . Both solutions give

$$\text{Vol}(M_{RL^2}) + i \text{CS}(M_{RL^2}) = 2.6667 \cdots - i \cdot 0.4112 \cdots.$$

## 4. 2-Bridge Links

### 4.1 Canonical Decomposition of 2-Bridge Link Complements

We briefly describe the canonical decomposition of a hyperbolic 2-bridge link. See [19] (also [10]) for details. We follow a notation of [19]. Let  $K_{q/p}$  be a hyperbolic 2-bridge knot or link (see, *e.g.*, [14] for the definition and the properties). Here we assume that  $p$  and  $q$  are coprime integers such that  $2 \leq q < p/2$ . When  $p$  is odd (resp. even),  $K_{q/p}$  is a knot (resp. a 2-component link). We use a continued fraction expression of  $q/p$ ,

$$q/p = \frac{1}{a_1 + \frac{1}{a_2 + \frac{1}{\ddots + \frac{1}{a_n}}}} = [a_1, a_2, \dots, a_n], \quad (4.1)$$

where  $n \geq 1$ ,  $a_j \in \mathbb{Z}_{>0}$ , and  $a_n \geq 2$ . We set

$$c = \sum_{i=1}^n a_i. \quad (4.2)$$

Correspondingly we have the chain of the Farey triangles,  $(\sigma[1], \sigma[2], \dots, \sigma[c])$  as in Fig. 9. The vertices of each Farey triangle are assigned with rational numbers,  $d_1/d_2$ ,  $d_3/d_4$ , and  $(d_1 + d_3)/(d_2 + d_4)$  with  $d_i \in \mathbb{Z}$ .

Each Farey triangle determines a triangulation of 4-punctured sphere  $\Sigma_{0,4} = (\mathbb{R}^2 \setminus \mathbb{Z}^2)/\Gamma$ , where  $\Gamma$  is a transformation group generated by  $\pi$ -rotations about every point



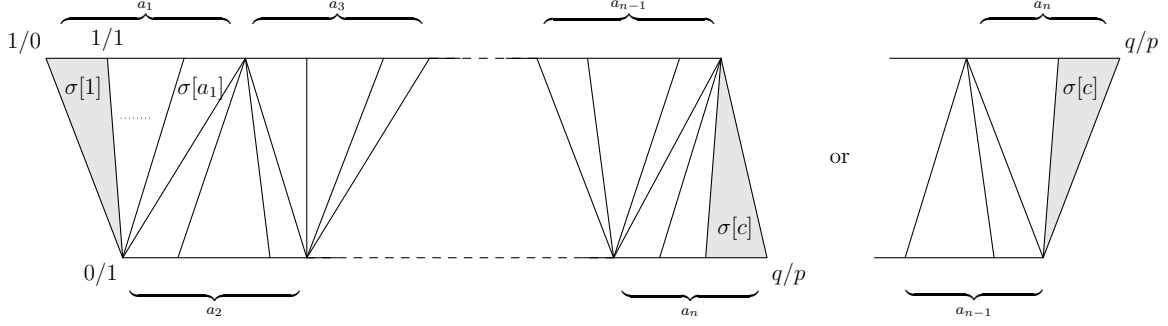


FIGURE 9. The Farey triangle

in  $\mathbb{Z}^2$ . When two Farey triangles  $\sigma[k]$  and  $\sigma[k+1]$  are adjacent, a flip connects triangulations of  $\Sigma_{0,4}$  as in Fig. 10. Namely when  $\sigma[k+1]$  is in the right (resp. left) to  $\sigma[k]$ , a flip  $R$  (resp.  $L$ ) acts on the triangulation of  $\Sigma_{0,4}$ . In constructing a canonical decomposition of the link complement  $S^3 \setminus K_{q/p}$ , the triangulations for the first Farey triangle  $\sigma[1]$  collapses into a single edge, and the Farey triangle  $\sigma[2]$  is folded along the edge of  $1/2$ . Similarly the triangle  $\sigma[c]$  collapses into an edge, and  $\sigma[c-1]$  is folded along the edge of  $[a_1, \dots, a_n - 2]$ . We use a sequence of symbols to denote these flips as [19]

$$F_1 F_2 \cdots F_{c-3} = \begin{cases} R^{a_1-1} L^{a_2} R^{a_3} \cdots R^{a_{n-1}} L^{a_n-2}, & \text{when } n \text{ is even,} \\ R^{a_1-1} L^{a_2} R^{a_3} \cdots L^{a_{n-1}} R^{a_n-2}, & \text{when } n \text{ is odd.} \end{cases} \quad (4.3)$$

Here  $F_k$  denotes a symbol,  $F_k = R$  or  $L$ , and acts on the triangulation for  $\sigma[k+1]$ .

As in the case of the once-punctured torus bundle, we can assign ideal hyperbolic tetrahedra to each flip. In the case of the four-punctured sphere  $\Sigma_{0,4}$ , a pair of ideal hyperbolic tetrahedra,  $\Delta_1(F_k)$  and  $\Delta_2(F_k)$ , are associated to the flip  $F_k$  as in Fig. 11. Here we have illustrated only a single peripheral annulus, since the combinatorics of four peripheral annuli are same. Due to the folding of  $\sigma[2]$ , the first pair of tetrahedra  $\Delta_i(F_1)$  is folded at the edge corresponding to  $1/2$ . Similarly the last pair of tetrahedra  $\Delta_i(F_{c-3})$  is also folded at the edge corresponding to  $[a_1, \dots, a_n - 2]$ .

## 4.2 $y$ -pattern and Hyperbolic Volume

We first formulate the flips (4.3) by use of the mutations in the  $y$ -variables. We set a triangulation of the four-punctured sphere  $\Sigma_{0,4}$  as in Fig. 10. It induces the cluster algebra of  $N = 6$  with the exchange matrix  $\mathbf{B}$

$$\mathbf{B} = \begin{pmatrix} 0 & 0 & -1 & -1 & 1 & 1 \\ 0 & 0 & -1 & -1 & 1 & 1 \\ 1 & 1 & 0 & 0 & -1 & -1 \\ 1 & 1 & 0 & 0 & -1 & -1 \\ -1 & -1 & 1 & 1 & 0 & 0 \\ -1 & -1 & 1 & 1 & 0 & 0 \end{pmatrix}, \quad (4.4)$$

whose quiver is in Fig. 12.

The flips,  $R$  and  $L$ , in Fig. 10, are simply identified with permuted mutations as

$$R = s_{5,6} s_{1,5} s_{2,6} \mu_1 \mu_2, \quad L = s_{5,6} s_{3,5} s_{4,6} \mu_3 \mu_4. \quad (4.5)$$

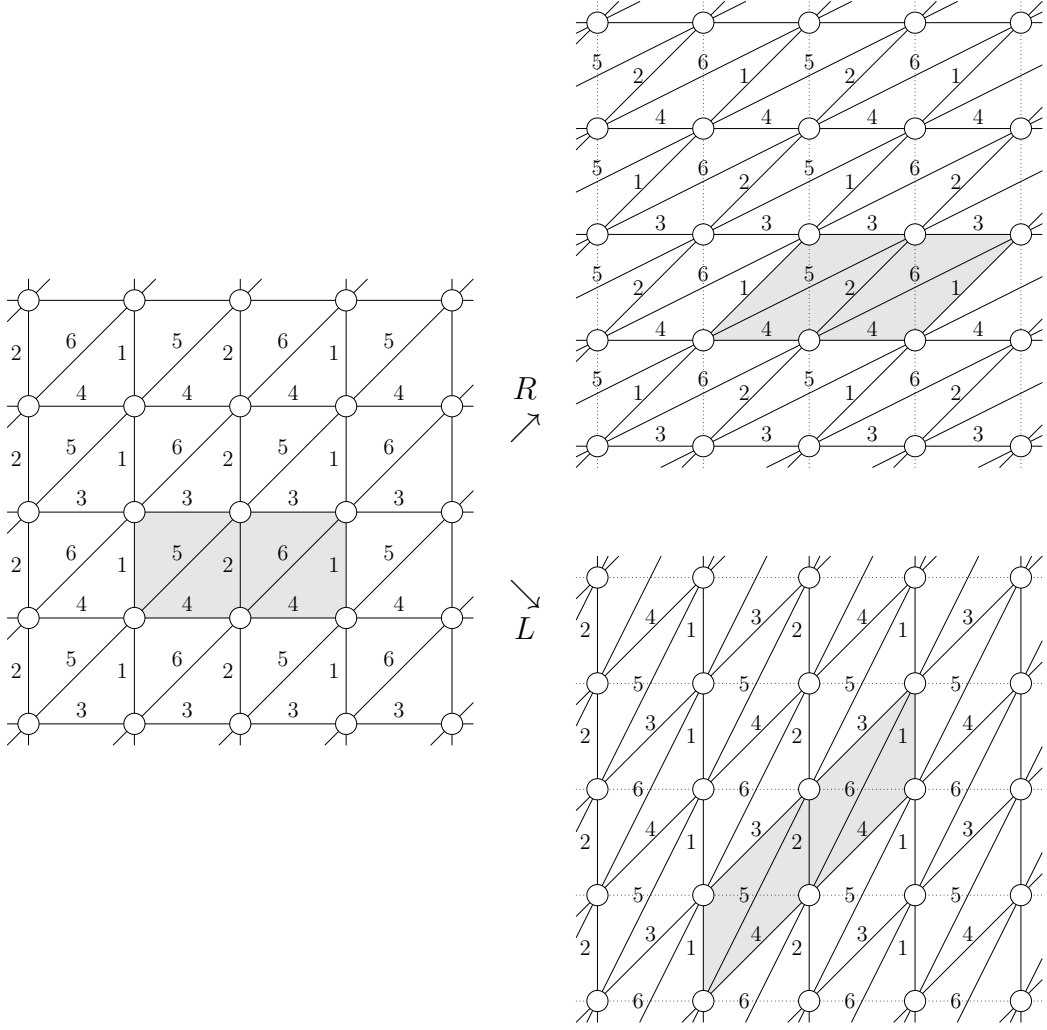


FIGURE 10. A triangulation of 4-punctured sphere  $\Sigma_{0,4}$  (left), where a fundamental region is colored gray. The flips of the triangulation are given in the right hand side.

Here, as in the case of the once-punctured torus, we have inserted the permutations  $s_{i,j}$  so that the exchange matrix  $\mathbf{B}$  (4.4) is invariant under  $R$  and  $L$ . Explicit actions on the  $y$ -variables are written as

$$(\mathbf{y}, \mathbf{B}) \xrightarrow{R} (R(\mathbf{y}), \mathbf{B}), \quad (\mathbf{y}, \mathbf{B}) \xrightarrow{L} (L(\mathbf{y}), \mathbf{B}), \quad (4.6)$$

where

$$R(\mathbf{y}) = \begin{pmatrix} y_5 (1 + y_1^{-1})^{-1} (1 + y_2^{-1})^{-1} \\ y_6 (1 + y_1^{-1})^{-1} (1 + y_2^{-1})^{-1} \\ y_3 (1 + y_1) (1 + y_2) \\ y_4 (1 + y_1) (1 + y_2) \\ y_2^{-1} \\ y_1^{-1} \end{pmatrix}^\top, \quad L(\mathbf{y}) = \begin{pmatrix} y_1 (1 + y_3^{-1})^{-1} (1 + y_4^{-1})^{-1} \\ y_2 (1 + y_3^{-1})^{-1} (1 + y_4^{-1})^{-1} \\ y_5 (1 + y_3) (1 + y_4) \\ y_6 (1 + y_3) (1 + y_4) \\ y_4^{-1} \\ y_3^{-1} \end{pmatrix}^\top. \quad (4.7)$$

**Definition 4.1.** A  $y$ -pattern for  $K_{q/p}$  is  $\mathbf{y}[k]$  for  $k = 1, 2, \dots, c - 2$  defined by

$$\mathbf{y}[k + 1] = F_k(\mathbf{y}[k]), \quad (4.8)$$

where  $F_k$  is  $R$  or  $L$  as in (4.3).

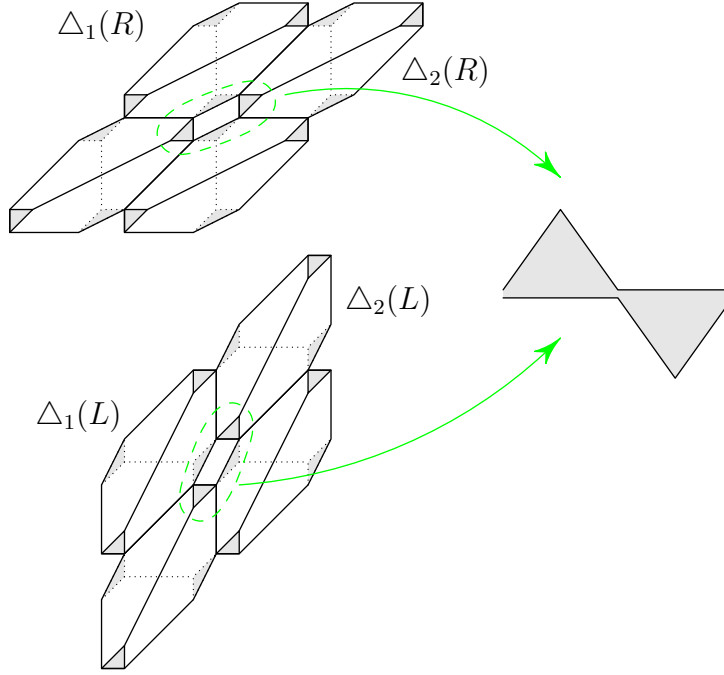


FIGURE 11. Left: The tetrahedra  $\Delta_i(R)$  and  $\Delta_i(L)$  assigned to the flip  $R$  and  $L$  on the four-punctured sphere  $\Sigma_{0,4}$  in Fig. 10. Right: Only a single peripheral annulus is illustrated.

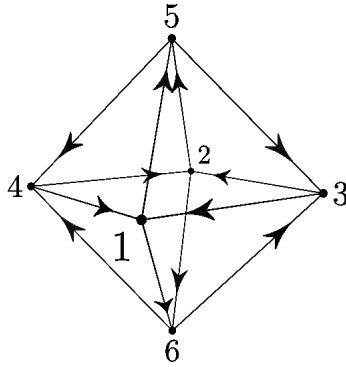


FIGURE 12. A quiver associated to the triangulation of the four-punctured sphere  $\Sigma_{0,4}$  in Fig. 10. The labeling of vertex corresponds to that of edge in Fig. 10.

**Proposition 4.2.** *Let  $\mathbf{y}[k]$  be a  $y$ -pattern for  $K_{q/p}$  constructed from an initial condition*

$$\mathbf{y}[1] = \left( y, y, -\frac{1}{y}, -\frac{1}{y}, -1, -1 \right). \tag{4.9}$$

*Here  $y$  is a solution of*

$$\begin{cases} y[c-2]_3 = y[c-2]_4 = -1, & \text{if } n \text{ is even,} \\ y[c-2]_1 = y[c-2]_2 = -1, & \text{if } n \text{ is odd,} \end{cases} \tag{4.10}$$

such that each modulus  $z_i[k]$  for  $i = 1, 2$  and  $k = 1, 2, \dots, c-3$  defined by

$$z_i[k] = \begin{cases} -\frac{1}{y[k]_i}, & \text{if } F_k = R, \\ -\frac{1}{y[k]_{2+i}}, & \text{if } F_k = L, \end{cases} \quad (4.11)$$

is in the upper half plane  $\mathbb{H}$ . Then  $z_i[k]$  denotes the modulus of the tetrahedron  $\Delta_i(F_k)$ .

*Remark 4.3.* See Appendix of [10], where proved is an existence of a geometric solution of (4.10). It is also announced in [1].

**Corollary 4.4.** *The hyperbolic volume of the link complement  $S^3 \setminus K_{q/p}$  is given by*

$$\text{Vol}(S^3 \setminus K_{q/p}) = \sum_{k=1}^{c-3} \sum_{i=1,2} D(z_i[k]), \quad (4.12)$$

where  $D(z)$  is the Bloch–Wigner function (2.9), and  $z_i[k]$ 's are the moduli (4.11).

*Remark 4.5.* Under the initial condition (4.9), we have invariants of  $y$ -variable under a mutation,

$$y[k]_{i_1} y[k]_{i_2} y[k]_{i_3} = 1, \quad (4.13)$$

for  $k = 1, 2, \dots, c-2$  and  $(i_1, i_2, i_3) \in \{1, 2\} \times \{3, 4\} \times \{5, 6\}$ .

### 4.3 Proof of Proposition 4.2

We shall check that the moduli  $z_i[k]$  of the ideal hyperbolic tetrahedra written in terms of the cluster  $y$ -variables as (4.11) fulfill both the gluing conditions and the completeness conditions by use of the developing map.

We study four cases separately,

(I) even  $n$ , and  $a_n > 2$ ,

$$F_1 \cdots F_{c-3} = R^{a_1-1} L^{a_2} \cdots L^{a_n-2}, \quad y[c-2]_3 = y[c-2]_4 = -1,$$

(II) even  $n$ , and  $a_n = 2$ ,

$$F_1 \cdots F_{c-3} = R^{a_1-1} L^{a_2} \cdots R^{a_n-1}, \quad y[c-2]_3 = y[c-2]_4 = -1,$$

(III) odd  $n$ , and  $a_n > 2$ ,

$$F_1 \cdots F_{c-3} = R^{a_1-1} L^{a_2} \cdots R^{a_n-2}, \quad y[c-2]_1 = y[c-2]_2 = -1,$$

(IV) odd  $n$ , and  $a_n = 2$ ,

$$F_1 \cdots F_{c-3} = R^{a_1-1} L^{a_2} \cdots L^{a_n-1}, \quad y[c-2]_1 = y[c-2]_2 = -1.$$

We start a proof for the case (I). We recall that the  $y$ -pattern is

$$\mathbf{y}[1] \xrightarrow{R} \cdots \xrightarrow{R} \mathbf{y}[a_1] \xrightarrow{L} \mathbf{y}[a_1+1] \xrightarrow{L} \cdots \xrightarrow{L} \mathbf{y}[a_1+a_2] \xrightarrow{R} \cdots$$

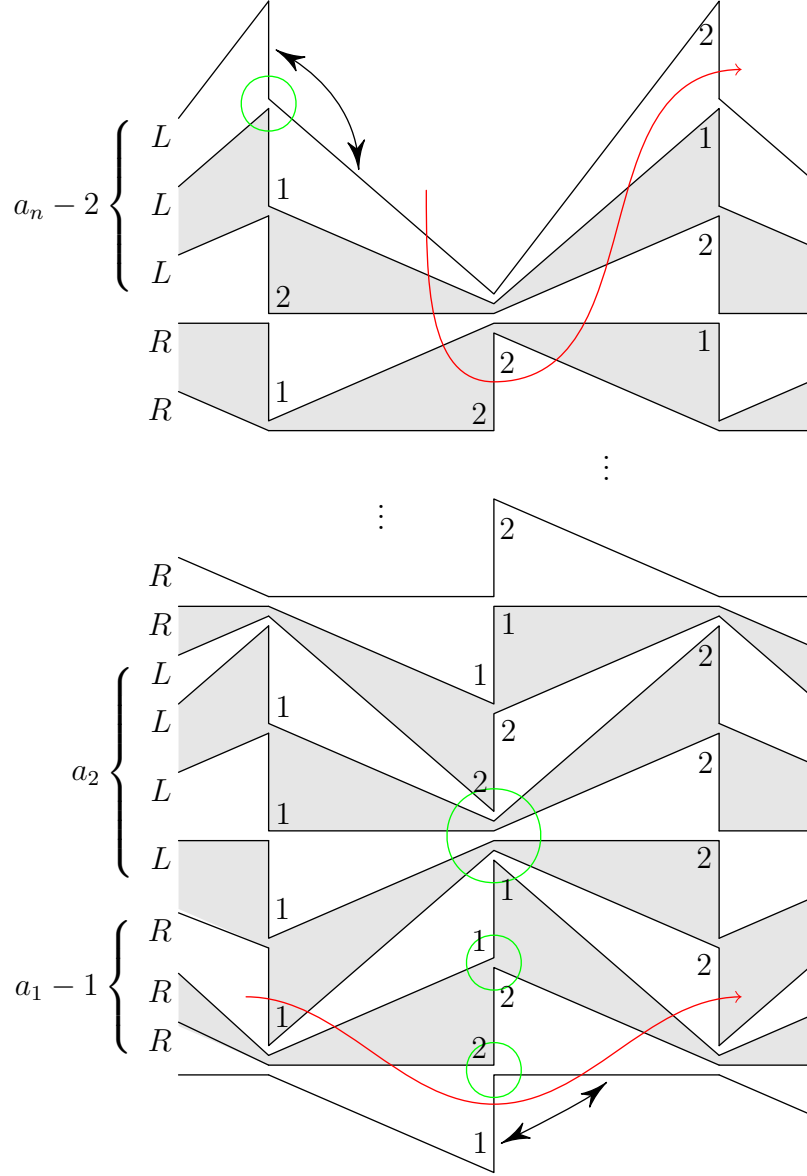


FIGURE 13. A developing map of one peripheral annulus for the case (I). Here  $R$  and  $L$  respectively denote tetrahedra  $\Delta_i(R)$  and  $\Delta_i(L)$  in Fig. 11. To emphasize the layered structure, each vertex is opened up and each layer is colored alternately. See Fig. 11. By 1 and 2 we denote dihedral angles  $z_1[k]$  and  $z_2[k]$  respectively. Two left-right-arrows denote an identification of edges, which are consequences of folding of  $\sigma[2]$  and  $\sigma[c - 1]$ .

A typical developing map of one peripheral annulus is depicted in Fig. 13. First of all, a gluing condition for a circle in the bottom of Fig. 13 can be checked as follows;

$$\begin{aligned} z_2[2] z_1''[1] z_2''[1] &= \frac{-1}{y[2]_2} \frac{1}{1 + y[1]_1^{-1}} \frac{1}{1 + y[1]_2^{-1}} \\ &= \frac{-1}{y[1]_6} = 1, \end{aligned}$$

where we have used  $\mathbf{y}[2] = R(\mathbf{y}[1])$  as given in (4.7), and the last equality is from (4.9). In the same manner, a gluing condition for the second circle from the bottom can be

checked by use of  $\mathbf{y}[3] = R(\mathbf{y}[2])$  and  $\mathbf{y}[2] = R(\mathbf{y}[1])$  as

$$\begin{aligned} z_1[3] z_1''[2] z_2''[2] z_2[1] &= \frac{1}{y[3]_1} \frac{1}{1 + y[2]_1^{-1}} \frac{1}{1 + y[2]_2^{-1}} \frac{1}{y[1]_2} \\ &= \frac{1}{y[2]_5 y[1]_2} = 1. \end{aligned}$$

We can check that  $z_1[k+1] z_1''[k] z_2''[k] z_2[k-1] = 1$ , and that this type of identity denotes a gluing condition composed from four angles in Fig. 13. A gluing condition for a circle in the middle of the figure is also checked as follows,

$$\begin{aligned} z_2[a_1 + a_2] \cdot \prod_{k=a_1-1}^{a_1+a_2-1} z_1''[k] z_2''[k] \cdot z_1[a_1 - 2] \\ &= \frac{1}{y[a_1 + a_2]_2} \cdot \prod_{k=a_1}^{a_1+a_2-1} \frac{1}{1 + y[k]_3^{-1}} \frac{1}{1 + y[k]_4^{-1}} \cdot \frac{1}{1 + y[a_1 - 1]_1^{-1}} \frac{1}{1 + y[a_1 - 1]_2^{-1}} \cdot \frac{1}{y[a_1 - 2]_1} \\ &= \frac{1}{y[a_1 + a_2]_2} \cdot \prod_{k=a_1}^{a_1+a_2-1} \frac{1}{1 + y[k]_3^{-1}} \frac{1}{1 + y[k]_4^{-1}} \cdot y[a_1]_2 \\ &= \frac{1}{y[a_1 + a_2]_2} y[a_1 + a_2]_2 = 1. \end{aligned}$$

Other gluing conditions can be checked by the similar computations.

A completeness condition can be read from curves in the figure. From the lower curve we have

$$\begin{aligned} z_1[a_1] \cdot \prod_{k=2}^{a_1-1} z_1'[k] z_2'[k] \cdot \frac{z_2'[1]}{z_1''[1]} &= \frac{-1}{y[a_1]_3} \cdot \prod_{k=2}^{a_1-1} (1 + y[k]_1) (1 + y[k]_2) \cdot \frac{1}{y[1]_1} \\ &= \frac{-1}{y[1]_1 y[1]_3} = 1, \end{aligned}$$

where we have used (4.9) in the last equality. It is noted that the completeness condition can also be checked from the upper curve in the figure as

$$\begin{aligned} \frac{z_1''[c-3]}{z_2'[c-3]} \cdot \prod_{k=c-a_n-1}^{c-4} z_1''[k] z_2''[k] \cdot z_2[c - a_n - 2] \\ &= -y[c-2]_2 y[c-2]_5 = 1, \end{aligned}$$

where (4.10) and (4.13) are used in the last equality.

This completes a proof for the case (I).

In the case (II), the developing map is slightly different from the case (I): the lower part of Fig. 13 is same, but an upper part is replaced with Fig. 14. A consistency check of gluing equations is similar to the case (I). For example, a gluing equation for a circle

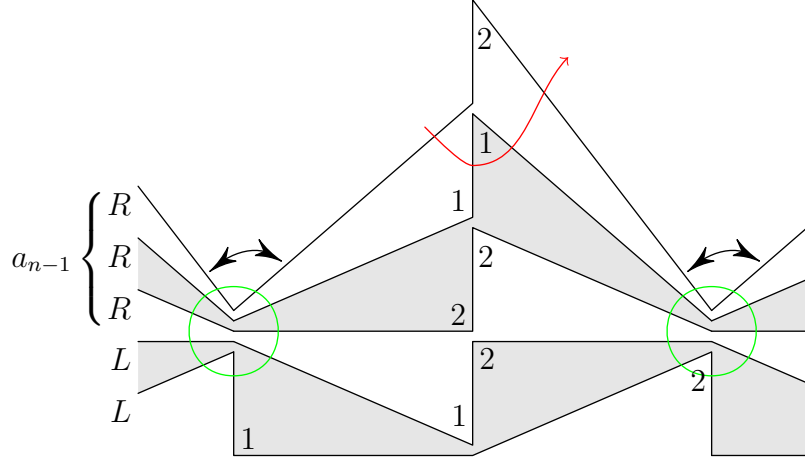


FIGURE 14. An upper part of developing map for the case (II).

in Fig. 14 is

$$\begin{aligned} & \prod_{k=c-a_{n-1}-1}^{c-3} z'_1[k] z'_2[k] \cdot z_2[c - a_{n-1} - 2] \\ &= \prod_{k=c-a_{n-1}}^{c-3} (1 + y[k]_1) (1 + y[k]_2) \cdot (1 + y[c - a_{n-1} - 1]_3) (1 + y[c - a_{n-1} - 1]_4) \frac{-1}{y[c - a_{n-1} - 2]_4} \\ &= -y[c - 2]_3 = 1, \end{aligned}$$

where the folding condition (4.10) is used in the last equality. A curve in Fig. 14 is read as

$$\frac{z''_1[c - 3]}{z'_2[c - 3]} z_1[c - 4] = -y[c - 2]_5 y[c - 2]_2 = 1,$$

where the last equality is a consequence of (4.10) and (4.13), and this denotes a completeness condition. This completes a proof for the case (II).

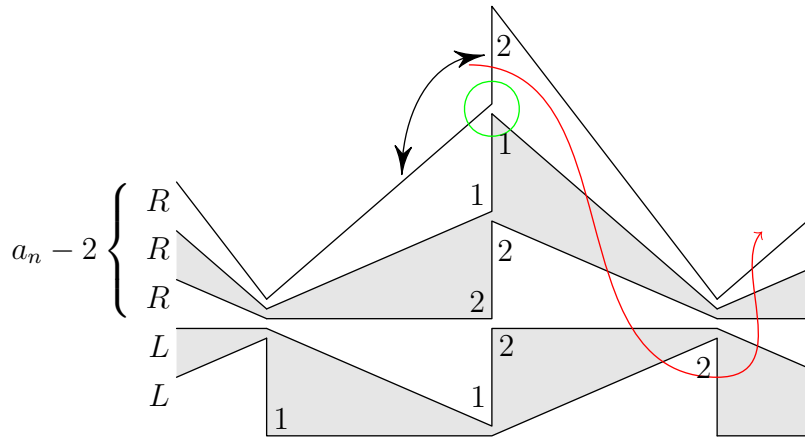


FIGURE 15. An upper part of developing map for the case (III).

In the case (III), an upper part of Fig. 13 is replaced with Fig. 15. A gluing condition for a circle in Fig. 15 can be checked as

$$\begin{aligned} z_1''[c-3] z_2''[c-3] z_1[c-4] &= (1 + y[c-3]_1^{-1})^{-1} (1 + y[c-3]_2^{-1})^{-1} \frac{-1}{y[c-4]_1} \\ &= -y[c-2]_2 = 1. \end{aligned}$$

Correspondingly a completeness condition is read from a curve in Fig. 15, and we can check

$$\frac{z_1'[c-3]}{z_2''[c-3]} \cdot \prod_{k=c-a_{n-1}}^{c-4} z_1'[k] z_2'[k] \cdot z_1[c-a_n-2] = -y[c-2]_6 y[c-2]_4 = 1,$$

by using (4.10) and (4.13) at the last equality. This completes a proof for the case (III).

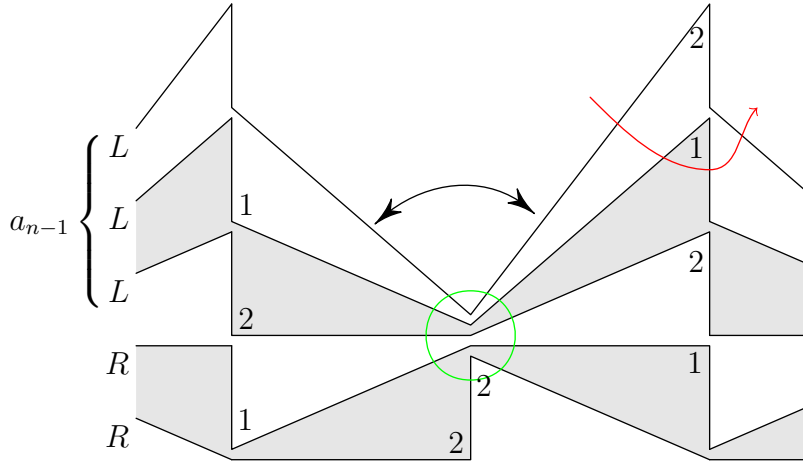


FIGURE 16. An upper part of developing map for case (IV).

In the last case (IV), an upper part of Fig. 13 is replaced by Fig. 16. A gluing condition for a curve in Fig. 16 is checked as

$$\begin{aligned} &\prod_{k=c-a_{n-1}-1}^{c-3} z_1''[k] z_2''[k] \cdot z_2[c-a_{n-1}-2] \\ &= \prod_{k=c-a_{n-1}}^{c-3} \frac{1}{1 + y[k]_3^{-1}} \frac{1}{1 + y[k]_4^{-1}} \cdot \frac{1}{1 + y[c-a_{n-1}-1]_1^{-1}} \frac{1}{1 + y[c-a_{n-1}-1]_2^{-1}} \frac{-1}{y[c-a_{n-1}-2]_2} \\ &= \prod_{k=c-a_{n-1}}^{c-3} (1 + y[k]_3^{-1})^{-1} (1 + y[k]_4^{-1})^{-1} \cdot (-y[c-a_{n-1}]_1) \\ &= -y[c-2]_1 = 1. \end{aligned}$$

Correspondingly we have a completeness condition corresponding to a curve,

$$\begin{aligned} \frac{z_1'[c-3]}{z_2''[c-3]} z_2[c-4] &= \frac{1 + y[c-3]_3}{y[c-3]_3} (1 + y[c-3]_4) \frac{-1}{y[c-4]_4} \\ &= -y[c-2]_3 y[c-2]_6 = 1, \end{aligned}$$

where we have used (4.10) and (4.13) at the last equality. This completes a proof for the case (IV).



To conclude, we have checked that both the gluing conditions and the completeness condition are fulfilled for every cases (I)–(IV).

#### 4.4 Cluster Pattern and Complex Volume

To study the complex volume of the complement of the 2-bridge link  $K_{q/p}$ , we reformulate the preceding result by use of the cluster variable  $\mathbf{x}$ . Recall that we use the tropical semifield in Def. 2.4 for the coefficient  $\varepsilon$ . Actions of the flips  $R$  and  $L$  defined as permuted cluster mutations (4.5) are explicitly given respectively by

$$(\mathbf{x}, \varepsilon) \xrightarrow{R} R(\mathbf{x}, \varepsilon), \quad (\mathbf{x}, \varepsilon) \xrightarrow{L} L(\mathbf{x}, \varepsilon), \quad (4.14)$$

where

$$R(\mathbf{x}, \varepsilon) = \left( \left( \begin{array}{c} x_5 \\ x_6 \\ x_3 \\ x_4 \\ \frac{\varepsilon_2}{1 \oplus \varepsilon_2} \frac{x_3 x_4}{x_2} + \frac{1}{1 \oplus \varepsilon_2} \frac{x_5 x_6}{x_2} \\ \frac{\varepsilon_1}{1 \oplus \varepsilon_1} \frac{x_3 x_4}{x_1} + \frac{1}{1 \oplus \varepsilon_1} \frac{x_5 x_6}{x_1} \end{array} \right)^\top, \left( \begin{array}{c} \varepsilon_5 \frac{\varepsilon_1}{1 \oplus \varepsilon_1} \frac{\varepsilon_2}{1 \oplus \varepsilon_2} \\ \varepsilon_6 \frac{\varepsilon_1}{1 \oplus \varepsilon_1} \frac{\varepsilon_2}{1 \oplus \varepsilon_2} \\ \varepsilon_3 (1 \oplus \varepsilon_1)(1 \oplus \varepsilon_2) \\ \varepsilon_4 (1 \oplus \varepsilon_1)(1 \oplus \varepsilon_2) \\ \varepsilon_2^{-1} \\ \varepsilon_1^{-1} \end{array} \right)^\top \right), \quad (4.15)$$

$$L(\mathbf{x}, \varepsilon) = \left( \left( \begin{array}{c} x_1 \\ x_2 \\ x_5 \\ x_6 \\ \frac{1}{1 \oplus \varepsilon_4} \frac{x_1 x_2}{x_4} + \frac{\varepsilon_4}{1 \oplus \varepsilon_4} \frac{x_5 x_6}{x_4} \\ \frac{1}{1 \oplus \varepsilon_3} \frac{x_1 x_2}{x_3} + \frac{\varepsilon_3}{1 \oplus \varepsilon_3} \frac{x_5 x_6}{x_3} \end{array} \right)^\top, \left( \begin{array}{c} \varepsilon_1 \frac{\varepsilon_3}{1 \oplus \varepsilon_3} \frac{\varepsilon_4}{1 \oplus \varepsilon_4} \\ \varepsilon_2 \frac{\varepsilon_3}{1 \oplus \varepsilon_3} \frac{\varepsilon_4}{1 \oplus \varepsilon_4} \\ \varepsilon_5 (1 \oplus \varepsilon_3)(1 \oplus \varepsilon_4) \\ \varepsilon_6 (1 \oplus \varepsilon_3)(1 \oplus \varepsilon_4) \\ \varepsilon_4^{-1} \\ \varepsilon_3^{-1} \end{array} \right)^\top \right).$$

**Definition 4.6.** A cluster pattern of  $K_{q/p}$  is  $(\mathbf{x}[k], \varepsilon[k])$  for  $k = 1, 2, \dots, c-2$  defined recursively by

$$(\mathbf{x}[k+1], \varepsilon[k+1]) = F_k(\mathbf{x}[k], \varepsilon[k]), \quad (4.16)$$

where  $F_k$  is  $R$  or  $L$  as (4.3).

Prop. 2.3 shows that the  $y$ -pattern  $\mathbf{y}[k]$  in Prop. 4.2 can be given in terms of the cluster pattern  $(\mathbf{x}[k], \varepsilon[k])$  as (2.4),

$$\mathbf{y}[k] = \left( \varepsilon[k]_1 \frac{x[k]_3 x[k]_4}{x[k]_5 x[k]_6}, \varepsilon[k]_2 \frac{x[k]_3 x[k]_4}{x[k]_5 x[k]_6}, \varepsilon[k]_3 \frac{x[k]_5 x[k]_6}{x[k]_1 x[k]_2}, \varepsilon[k]_4 \frac{x[k]_5 x[k]_6}{x[k]_1 x[k]_2}, \varepsilon[k]_5 \frac{x[k]_1 x[k]_2}{x[k]_3 x[k]_4}, \varepsilon[k]_6 \frac{x[k]_1 x[k]_2}{x[k]_3 x[k]_4} \right). \quad (4.17)$$

The conditions (4.9) and (4.10) for the  $y$ -variables, which come from the folding of the Farey triangles  $\sigma[2]$  and  $\sigma[c-1]$ , are fulfilled when we suppose the following constraints

on the cluster variables  $\mathbf{x}[k]$  and the coefficients  $\boldsymbol{\varepsilon}[k]$ :

$$\psi(\boldsymbol{\varepsilon}[1]) = (-1, -1, 1, 1, -1, -1), \quad \text{or} \quad (1, 1, -1, -1, -1, -1), \quad (4.18)$$

$$\mathbf{x}[1] = (x, x, x, x, x_5, x_6), \quad (4.19)$$

and

$$\begin{cases} \psi(\boldsymbol{\varepsilon}[c-2]_3) = \psi(\boldsymbol{\varepsilon}[c-2]_4) = -1, & \text{if } n \text{ is even,} \\ \psi(\boldsymbol{\varepsilon}[c-2]_2) = \psi(\boldsymbol{\varepsilon}[c-2]_1) = -1, & \text{if } n \text{ is odd,} \end{cases} \quad (4.20)$$

$$\begin{cases} x[c-2]_1 = x[c-2]_2 = x[c-2]_5 = x[c-2]_6, & \text{if } n \text{ is even,} \\ x[c-2]_3 = x[c-2]_4 = x[c-2]_5 = x[c-2]_6, & \text{if } n \text{ is odd.} \end{cases} \quad (4.21)$$

The initial cluster  $x$ -variable (4.19) means that the edges for  $x_1, x_2, x_3$ , and  $x_4$  are identified. Here  $\psi$  is defined in Def. 2.5. At (4.21) and in the rest of this section, the coefficient  $\boldsymbol{\varepsilon}[k]_i$  in the cluster variable  $x[k]_i$  are set to be  $+1$  or  $-1$  by acting the map  $\psi$ . We should note that one of the two conditions (4.18) is chosen so that it is consistent with the constraint (4.20). To fulfill (4.18), we set

$$\boldsymbol{\varepsilon}[1] = (\delta^{m_1}, \delta^{m_1}, \delta^{m_2}, \delta^{m_2}, \delta^{m_3}, \delta^{m_3}),$$

where  $(m_1, m_2, m_3)$  is (odd, even, odd) (resp. (even, odd, odd)) for the first (resp. second) case. By these conditions, the cluster variables  $x[k]_j$  are solved up to constant. We can see from the three-dimensional interpretation of the flips in Fig. 11 that the cluster variables  $x[k]_j$  are assigned to edges of the ideal tetrahedra  $\Delta_i(F_k)$ , and that both (4.19) and (4.21) imply that the identified edges in  $S^3 \setminus K_{q/p}$  have equal complex numbers. Then the cluster variables are identified with Zickert's complex variables on edges, and the complex volume can be computed from the cluster variables.

To compute the complex volume modulo  $\pi^2$ , we should fix an orientation of each ideal tetrahedra  $\Delta_i(F_k)$ . Although, unlike the case of the once-punctured torus bundle, an orientation of triangulations of  $\Sigma_{0,4}$  cannot be fixed uniquely due to the transformation group  $\Gamma$ , and it is tedious to give orientations from  $q/p$ . So for simplicity, we discard a vertex ordering, and we give a formula of the complex volume modulo  $\frac{\pi^2}{6}$ . From (4.11) and (4.17), we obtain the following.

**Lemma 4.7.** *Let  $(\mathbf{x}[k], \boldsymbol{\varepsilon}[k])$  be a cluster pattern which satisfies the conditions (4.18)–(4.21). Then the moduli  $z_1[k]$  and  $z_2[k]$  of a pair of tetrahedra  $\Delta_1(F_k)$  and  $\Delta_2(F_k)$  are given from the cluster pattern,*

$$z_i[k] = \begin{cases} -\frac{1}{\boldsymbol{\varepsilon}[k]_i} \frac{x[k]_5 x[k]_6}{x[k]_3 x[k]_4}, & \text{for } F_k = R, \\ -\frac{1}{\boldsymbol{\varepsilon}[k]_{2+i}} \frac{x[k]_1 x[k]_2}{x[k]_5 x[k]_6}, & \text{for } F_k = L. \end{cases} \quad (4.22)$$

for  $k = 1, \dots, c-2$  and  $i = 1, 2$ .

We choose  $x$ -variable such that the  $y$ -variables are geometric. See Remark 4.3. Then we can identify the  $x$ -variables with the edge parameters  $c_{ab}$ , and we obtain the flattenings of the tetrahedra  $\Delta_i(F_k)$  as follows.

**Lemma 4.8.** *We follow the setting of Lemma 4.7. The flattenings  $(z_i[k]; p_i[k], q_i[k])$  for the tetrahedron  $\Delta_i(F_k)$  are given by*

$$\begin{aligned} \log z_i[k] + p_i[k] \pi i &= \begin{cases} \log x[k]_5 + \log x[k]_6 - \log x[k]_3 - \log x[k]_4, & \text{for } F_k = R, \\ \log x[k]_1 + \log x[k]_2 - \log x[k]_5 - \log x[k]_6, & \text{for } F_k = L, \end{cases} \\ -\log(1 - z_i[k]) + q_i[k] \pi i &= \begin{cases} \log x[k]_3 + \log x[k]_4 - \log x[k]_i - \log x[k+1]_{7-i}, & \text{for } F_k = R. \\ \log x[k]_5 + \log x[k]_6 - \log x[k]_{2+i} - \log x[k+1]_{7-i}, & \text{for } F_k = L, \end{cases} \end{aligned} \quad (4.23)$$

for  $k = 1 \cdots, c-2$  and  $i = 1, 2$ .

*Proof.* Due to (4.15), we have

$$\frac{1}{1 - z_i[k]} = \begin{cases} \frac{\varepsilon[k]_i}{1 \oplus \varepsilon[k]_i} \frac{x[k]_3 x[k]_4}{x[k]_i x[k+1]_{7-i}}, & \text{for } F_k = R, \\ \frac{\varepsilon[k]_{2+i}}{1 \oplus \varepsilon[k]_{2+i}} \frac{x[k]_5 x[k]_6}{x[k]_{2+i} x[k+1]_{7-i}} & \text{for } F_k = L, \end{cases} \quad (4.24)$$

for  $i = 1, 2$ . By comparing (4.22) and (4.24) with (2.15), we get the claim.  $\square$

It is straightforward to get the following theorem from these Lemmas.

**Theorem 4.9.** *The complex volume of the 2-bridge link complement  $S^3 \setminus K_{q/p}$  is given by the flattenings of Lemma 4.8 as*

$$i (\text{Vol}(S^3 \setminus K_{q/p}) + i \text{CS}(S^3 \setminus K_{q/p})) = \sum_{k=1}^{c-3} \sum_{i=1,2} \widehat{L}(z_i[k]; p_i[k], q_i[k]) \pmod{\frac{\pi^2}{6}}. \quad (4.25)$$

*Remark 4.10.* The orientation of each tetrahedron can be determined case by case. As an example, we study  $K_{[a+1,2]}$ , which has a cluster pattern

$$(\mathbf{x}[1], \boldsymbol{\varepsilon}[1]) \xrightarrow{R} (\mathbf{x}[2], \boldsymbol{\varepsilon}[2]) \xrightarrow{R} \cdots \xrightarrow{R} (\mathbf{x}[a+1], \boldsymbol{\varepsilon}[a+1]).$$

Based on triangulations of link complements, we may choose vertex ordering so that

$$(\text{sgn}(\Delta_1(F_k)), \text{sgn}(\Delta_2(F_k))) = \begin{cases} (-1, -1), & \text{for odd } k \text{ and } k \neq a, a-1, \\ (+1, +1), & \text{for even } k \text{ and } k \neq a, \\ (+1, -1), & \text{for odd } k \text{ and } k = a, a-1, \\ (-1, -1), & \text{for even } k \text{ and } k = a. \end{cases}$$

We can then identify

$$\begin{aligned}
& (z_1[k], z_2[k]) \\
&= \begin{cases} \left( \frac{1 \oplus \varepsilon[k]_1}{\varepsilon[k]_1} \frac{x[k]_1 x[k+1]_6}{x[k]_3 x[k]_4}, \frac{1 \oplus \varepsilon[k]_2}{\varepsilon[k]_2} \frac{x[k]_2 x[k+1]_5}{x[k]_3 x[k]_4} \right), & \text{for odd } k \text{ and } k \neq a, a-1, \\ \left( -\frac{1}{\varepsilon[k]_1} \frac{x[k]_5 x[k]_6}{x[k]_3 x[k]_4}, -\frac{1}{\varepsilon[k]_2} \frac{x[k]_5 x[k]_6}{x[k]_3 x[k]_4} \right), & \text{for even } k \text{ and } k \neq a, \\ \left( (1 \oplus \varepsilon[k]_1) \frac{x[k]_1 x[k+1]_6}{x[k]_5 x[k]_6}, \frac{1 \oplus \varepsilon[k]_2}{\varepsilon[k]_2} \frac{x[k]_2 x[k+1]_5}{x[k]_3 x[k]_4} \right), & \text{for odd } k \text{ and } k = a, a-1, \\ \left( \frac{1}{1 \oplus \varepsilon[k]_1} \frac{x[k]_5 x[k]_6}{x[k]_1 x[k+1]_6}, \frac{1}{1 \oplus \varepsilon[k]_2} \frac{x[k]_5 x[k]_6}{x[k]_2 x[k+1]_5} \right), & \text{for even } k \text{ and } k = a. \end{cases}
\end{aligned} \tag{4.26}$$

Accordingly, we have

$$\begin{aligned}
& \left( \frac{1}{1 - z_1[k]}, \frac{1}{1 - z_2[k]} \right) \\
&= \begin{cases} \left( -\varepsilon[k]_1 \frac{x[k]_3 x[k]_4}{x[k]_5 x[k]_6}, -\varepsilon[k]_2 \frac{x[k]_3 x[k]_4}{x[k]_5 x[k]_6} \right), & \text{for odd } k \text{ and } k \neq a, a-1, \\ \left( \frac{\varepsilon[k]_1}{1 \oplus \varepsilon[k]_1} \frac{x[k]_3 x[k]_4}{x[k]_1 x[k+1]_6}, \frac{\varepsilon[k]_2}{1 \oplus \varepsilon[k]_2} \frac{x[k]_3 x[k]_4}{x[k]_2 x[k+1]_5} \right), & \text{for even } k \text{ and } k \neq a, \\ \left( -\frac{1}{\varepsilon[k]_1} \frac{x[k]_5 x[k]_6}{x[k]_3 x[k]_4}, -\varepsilon[k]_2 \frac{x[k]_3 x[k]_4}{x[k]_5 x[k]_6} \right), & \text{for odd } k \text{ and } k = a, a-1, \\ \left( \frac{1 \oplus \varepsilon[k]_1}{\varepsilon[k]_1} \frac{x[k]_1 x[k+1]_6}{x[k]_3 x[k]_4}, \frac{1 \oplus \varepsilon[k]_2}{\varepsilon[k]_2} \frac{x[k]_2 x[k+1]_5}{x[k]_3 x[k]_4} \right), & \text{for even } k \text{ and } k = a. \end{cases}
\end{aligned} \tag{4.27}$$

These data give the flattening  $(z_i[k]; p_i[k], q_i[k])$  for each tetrahedron from (2.15), and we get

$$\begin{aligned}
& i (\text{Vol}(S^3 \setminus K_{[a+1,2]}) + i \text{CS}(S^3 \setminus K_{[a+1,2]})) \\
&= \sum_{k=1}^a \sum_{i=1,2} \text{sgn}(\Delta_i(F_k)) \widehat{L}(z_i[k]; p_i[k], q_i[k]) \pmod{\pi^2}.
\end{aligned} \tag{4.28}$$

#### 4.5 Example: $6_1$

The knot  $6_1$  is a two-bridge knot  $K_{[4,2]}$ , which corresponds to  $a = 3$  in Remark 4.10. When we set an initial seed as

$$\mathbf{x}[1] = (1, 1, 1, 1, x, x), \quad \boldsymbol{\varepsilon}[1] = (\delta^0, \delta^0, \delta^1, \delta^1, \delta^1, \delta^1),$$

the constraint (4.21) is read as

$$x(2 + x^2) = 1 + 3x^2 + x^4.$$

A geometric solution is  $x = 0.1048 \cdots - i \cdot 1.5524 \cdots$ , and the flattenings are calculated from (4.26) and (4.27) to be

$k$	$(z_1[k], z_2[k])$	$(p_1[k], p_2[k])$	$(q_1[k], q_2[k])$
1	$(-1.3992 \cdots - i \cdot 0.3256 \cdots, -1.3992 \cdots - i \cdot 0.3256 \cdots)$	$(0, 0)$	$(1, 1)$
2	$(1.8518 \cdots + i \cdot 0.9112 \cdots, 1.8518 \cdots + i \cdot 0.9112 \cdots)$	$(-2, -2)$	$(-1, -1)$
3	$(0.8951 \cdots + i \cdot 1.552 \cdots, 0.9566 \cdots - i \cdot 0.6412 \cdots)$	$(-2, 0)$	$(1, -1)$

We get from (4.28)

$$\text{Vol}(S^3 \setminus 6_1) + i \text{CS}(S^3 \setminus 6_1) = 3.1639 \cdots + i \cdot 3.0788 \cdots \in \mathbb{C}/i\pi^2 \mathbb{Z},$$

which coincides with the known result [2].

### Acknowledgments

One of the authors (KH) thanks T. Dimofte and J. Murakami for communications. He also thanks to participants of the workshop “Low-Dimensional Topology and Number Theory” at MFO in 2012. Thanks are also to M. Sakuma for comments on ideal triangulations. The work of KH is supported in part by JSPS KAKENHI Grant Number 23340115, 24654041, 22540069. RI is partially supported by Grant-in-Aid for Young Scientists (B) (22740111).

### References

- [1] H. Akiyoshi, M. Sakuma, M. Wada, and Y. Yamashita, *Punctured Torus Groups and 2-Bridge Knot Groups (I)*, Lecture Notes in Math. **1909**, Springer, Berlin, 2007.
- [2] M. Culler, N.M. Dunfield, and J.R. Weeks, *SnapPy, a computer program for studying the geometry and topology of 3-manifolds*, <http://snappy.computop.org>
- [3] T. Dimofte, S. Gukov, J. Lenells, and D. Zagier, *Exact results for perturbative Chern–Simons theory with complex gauge group*, Commun. Number Theory Phys. **3**, 363–443 (2009).
- [4] W. Floyd and A. Hatcher, *Incompressible surfaces in punctured torus bundles*, Topology Appl. **13**, 263–282 (1982).
- [5] V. V. Fock and A. B. Goncharov, *Moduli spaces of local systems and higher Teichmüller theory*, Publ. Math. Inst. Hautes Études Sci. **103**, 1–211 (2006), [math/0311149](#).
- [6] S. Fomin, M. Shapiro, and D. Thurston, *Cluster algebras and triangulated surfaces I. cluster complexes*, Acta Math. **201**, 83–146 (2008), [math/0608367](#).
- [7] S. Fomin and D. Thurston, *Cluster algebras and triangulated surfaces II. lambda lengths*, preprint (2012), [arXiv:1210.5569 \[math.GT\]](#).
- [8] S. Fomin and A. Zelevinsky, *Cluster algebras I. foundations*, J. Amer. Math. Soc. **15**, 497–529 (2002), [math/0104151](#).
- [9] ———, *Cluster algebras IV: coefficients*, Composito Math. **143**, 112–164 (2007), [math/0602259](#).

- [10] F. Guéritaud, *On canonical triangulations of once-punctured torus bundles and two-bridge link complements*, *Geom. Topol.* **10**, 1239–1284 (2006), with an appendix by D. Futer, [math/0406242](#).
- [11] K. Hikami, *Generalized volume conjecture and the  $A$ -polynomial — the Neumann–Zagier potential function as a classical limit of partition function*, *J. Geom. Phys.* **57**, 1895–1940 (2007), [math/0604094](#).
- [12] R. M. Kashaev, *The hyperbolic volume of knots from quantum dilogarithm*, *Lett. Math. Phys.* **39**, 269–275 (1997), [q-alg/9601025](#).
- [13] H. Murakami and J. Murakami, *The colored Jones polynomials and the simplicial volume of a knot*, *Acta Math.* **186**, 85–104 (2001), [math/9905075](#).
- [14] K. Murasugi, *Knot Theory and Its Applications*, Birkhäuser, 1996.
- [15] K. Nagao, Y. Terashima, and M. Yamazaki, *Hyperbolic geometry and cluster algebra*, preprint (2011), [arXiv:1112.3106](#) [[math.GT](#)].
- [16] W. D. Neumann, *Combinatorics of triangulations and the Chern–Simons invariant for hyperbolic 3-manifolds*, in B. Apanasov, W. D. Neumann, A. W. Reid, and L. Siebenmann, eds., *Topology '90*, vol. 1 of *Ohio State Univ. Math. Res. Inst. Publ.*, pp. 243–271, de Gruyter, Berlin, 1992.
- [17] ———, *Extended Bloch group and the Cheeger–Chern–Simons class*, *Geom. Topol.* **8**, 413–474 (2004).
- [18] W. D. Neumann and D. Zagier, *Volumes of hyperbolic three-manifolds*, *Topology* **24**, 307–332 (1985).
- [19] M. Sakuma and J. Weeks, *Examples of canonical decompositions of hyperbolic link complements*, *Japan J. Math.* **21**, 393–439 (1995).
- [20] Y. Terashima and M. Yamazaki, *Semiclassical analysis of the 3d/3d relation*, preprint (2011), [arXiv:1106.3066](#) [[hep-th](#)].
- [21] W. P. Thurston, *The geometry and topology of three-manifolds*, Lecture Notes in Princeton University, Princeton (1980).
- [22] D. Zagier, *The dilogarithm function*, in P. Cartier, B. Julia, P. Moussa, and P. Vanhove, eds., *Frontiers in Number Theory, Physics, and Geometry II. On Conformal Field Theories, Discrete Groups and Renormalization*, pp. 3–65, Springer, Berlin, 2007.
- [23] C. K. Zickert, *The volume and Chern–Simons invariant of a representation*, *Duke Math. J.* **150**, 489–532 (2009), [arXiv:0710.2049](#) [[math.GT](#)].

FACULTY OF MATHEMATICS, KYUSHU UNIVERSITY, FUKUOKA 819-0395, JAPAN.

*E-mail address:* [KHikami@gmail.com](mailto:KHikami@gmail.com)

DEPARTMENT OF MATHEMATICS AND INFORMATICS, FACULTY OF SCIENCE, CHIBA UNIVERSITY, CHIBA 263-8522, JAPAN.

*E-mail address:* [reiiy@math.s.chiba-u.ac.jp](mailto:reiiy@math.s.chiba-u.ac.jp)

